

A time-dependent model of generator failures and recoveries captures correlated events and quantifies temperature dependence

Sinnott Murphy^a, Fallaw Sowell^b, Jay Apt^{a,b,*}

^a Department of Engineering & Public Policy, Carnegie Mellon University, Pittsburgh, PA, USA

^b Tepper School of Business, Carnegie Mellon University, Pittsburgh, PA, USA

HIGHLIGHTS

- We quantify the temperature dependence of forced outages for six generator types.
- Generator transition probabilities are modeled using logistic regression.
- Nonhomogeneous Markov models capture observed correlated generator failures.
- Resource adequacy can be improved by accounting for temperature dependence.

ARTICLE INFO

Keywords:

Resource adequacy
Generating availability data system
Correlated failures
Nonhomogeneous Markov model
Logistic regression

ABSTRACT

Most current approaches to resource adequacy modeling assume that each generator in a power system fails and recovers independently of other generators with invariant transition probabilities. This assumption has been shown to be wrong. Here we present a new statistical model that allows generator failure models to incorporate correlated failures and recoveries. In the model, transition probabilities are a function of exogenous variables; as an example we use temperature and system load. Model parameters are estimated using 23 years of data for 1845 generators in the USA's largest electricity market. We show that temperature dependencies are statistically significant in all generator types, but are most pronounced for diesel and natural gas generators at low temperatures and nuclear generators at high temperatures. Our approach yields significant improvements in predictive performance compared to current practice, suggesting that explicit models of generator transitions using jointly experienced stressors can help grid planners more precisely manage their systems.

1. Introduction

Grid planners procure enough electric power generation to meet predicted demand and reserve generation to cover the statistical chance that one or more generators will fail. The process of determining how much generation to procure is called resource adequacy modeling (RAM). It is well known that severe environmental conditions can lead to elevated failure probabilities for power system components [1–3]. PJM, a large system operator in the USA, documents generator outage rates three times the historical winter average during the January 2014 Polar Vortex event [2]; and generator outage rates nearly twice the historical winter average during a milder cold snap that occurred in January 2018 [3]. Yet most current approaches to resource adequacy

modeling are unable to account for these risks because they treat generators as homogeneous Markov models (i.e., having time-invariant transition probabilities) [1,4–7].¹

This assumption is inconsistent with results from recent empirical work using four years of Generating Availability Data System (GADS) data from the North American Electric Reliability Corporation (NERC) that demonstrated the existence of correlated failures in most NERC reliability regions [8]. The correlated failures demonstrated in [8] are consistent with a numerical example presented by Gaver et al. [1] that shows much higher reliability adverse effects under adverse weather conditions. The observation that generators fail simultaneously leaves open the question of how to model correlated failures and recoveries. Severe environmental conditions experienced by many generators

* Corresponding author.

E-mail addresses: sjmurphy@andrew.cmu.edu (S. Murphy), fs0v@andrew.cmu.edu (F. Sowell), apt@cmu.edu (J. Apt).

¹ Standard RAM practice in the U.S. is as follows. First, the most recent five years of historical availability data are used to calculate an availability statistic for each generator. Second, the availability statistics are combined to calculate a distribution of available capacity for a future planning year for the power system. RAM assumes that the availability statistic corresponds to the generator's probability of being unavailable due to an unscheduled failure in every hour of the planning year.

Nomenclature			
<i>Symbols</i>		P_i	probability of the generator remaining derated in the next hour when it is currently derated
A	available state of two-state Markov model	Q_i	probability of the generator remaining available in the next hour when it is currently available
AA	available-to-available transition	X_i	vector of covariate observations
AD	available-to-derated transition	<i>Abbreviations and acronyms</i>	
α_i	equals 1 if the i^{th} observation used to fit the available model is AA, and 0 otherwise	C	celsius
β_A, β_D	parameter vectors for the available and derated models, respectively	CC	combined cycle gas generator
D	derated state of two-state Markov model	CT	simple cycle gas generator (combustion turbine)
DA	derated-to-available transition	DS	diesel generator
DD	derated-to-derated transition	eGRID	emissions and Generation Resource Integrated Database
Δ_i	equals 1 if the i^{th} observation used to fit the derated model is DD, and 0 otherwise	GADS	generating Availability Data System
EFDH	equivalent forced derating hours, the sum of hours where the generator experiences a forced derating, reported in full-outage-equivalent hours	GW	Gigawatts
EFOF	equivalent forced outage factor, a common availability statistic	HD	hydroelectric or pumped storage generator
FOH	forced outage hours, the sum of hours where the generator experiences a forced outage	IEEE	institute of Electrical and Electronics Engineers
$\mathcal{L}(\cdot)$	likelihood function	NERC	north American Electric Reliability Corporation, the electric reliability organization for the United States
PH	period hours, total number of hours in the calculation period of interest	NU	nuclear generator
		PJM	the PJM Interconnection, an independent system operator / regional transmission organization in the mid-Atlantic United States
		RAM	resource adequacy modeling
		ST	steam turbine generator (used equivalently as coal generator in PJM)

simultaneously is one possible explanation of these results.

Here we test this possibility with a time-varying (nonhomogeneous) Markov model fit using 23 years of data for 1845 generators in the USA's largest electricity market. The nonhomogeneous Markov model's probabilities of transitioning, e.g. from fully available to partially or fully derated, depend on exogenous variables such as temperature and system load (the electric energy being used by customers). Many factors could affect transition probabilities. However, if failures (transitions from working to not working) depend on variables that are jointly experienced by many generators, such an approach could capture the observed correlated failures. Understanding the causes of correlated failures and recoveries can help in the procurement of reserves, payments for which amount to billions of dollars per year in the USA [9].

Markov models are widely used in power system reliability analyses. The traditional two-state model assumes generators are either fully available or fully unavailable [10,11]. Common generalizations allow additional states [12], different two-state models over a discrete set of environments: e.g. "normal weather" versus "adverse weather" [1,13–15], or generator "in demand" versus "not in demand" [16–18]. Billinton and Bollinger [13] derive steady-state probability distributions for one-, two-, and three-line transmission systems. Liu and Singh [14] use Bayesian networks to study common-cause and independent failures due to hurricanes in a composite power system. Billinton and Li [15] allow segments of a single transmission line to experience different weather states so as to not over-estimate failure bunching in power systems that cover large geographic areas. Bhavaraju et al. [16] use a generalizable multi-state homogeneous Markov model to develop steady-state probability distributions for peaking generators; Billinton and Chowdhury [17] employ a three-state model. An IEEE task group [18] describes multiple models incorporating "in demand" versus "not in demand" states to improve upon the traditional two-state models for estimating the probability of being unavailable when needed by the system for peaking generators.

Particularly with respect to transmission and distribution system reliability, there has been significant scholarly attention to the effects of extreme weather and natural disasters [19–23]. Bramer et al. [19]

develop penalized logistic regression models to predict grid stress as a function of a suite of weather variables in the eastern USA. Li et al. [20] evaluates the hazard effects of wind storms on distribution systems in the northeastern USA using multiple metrics including system average interruption frequency index (SAIFI), system average interruption duration index (SAIDI), and expected energy not supplied (EENS). Bernstein et al. [21] develop a cascading transmission line outage model that allows for non-proximate line failures using the network topology of the western USA. Panteli and Mancarella [22] use a sequential Monte Carlo simulation-based time series simulation model to capture the effect of weather dependent failure probabilities on a six-bus system. Wei et al. [23] model distribution failures in the eastern USA during Hurricane Ike using a Poisson process estimated using observed failure data.

Homogeneous Markov models are most commonly employed, which means that transition probabilities are constant [10,24]. To model correlated failures, a new state must be created for each combination of generators failing simultaneously [25–27]; the state space therefore grows geometrically as the number of generators increases. While this approach can be successfully used to model multiple generators in a power plant or a small number of transmission lines, the intractability of applying it to a fleet of generators in a large power system has led researchers to define states in terms of system capabilities or to merge states [28,29]. Hou et al. [29] use a continuous time Markov chain where higher-order outage states are merged to improve tractability of a bottom-up reliability assessment of a composite generation and transmission power system. Felder [28] instead proposes a top-down model where system states are defined based on system capabilities rather than component states. Computing transition probabilities that depend on variables such as temperature and load to capture correlated failures can require long time series of generator-level data; these data were not previously available.

Using these generator-level data, we model each generator with only two states, but allow transition probabilities to depend on exogenous variables such as temperature. Similar approaches have been employed to study distribution and transmission system reliability

[23,30–32], but to our knowledge none have been used to study correlated generator failures in a large power system. Andreasson [30] examines the implications of correlated transmission line failures for risk of load shed to a 470-bus model of the Nordic power system. Wang et al. [31] allow failure rates of transmission lines to vary by season to account for failures caused by meteorological events. Ertekin et al. [32] model distribution system failures in New York City as a non-homogeneous Poisson process accounting for maintenance and other line features. To conduct this analysis we create hourly time series of transitions for 1845 generators in the eastern USA using 23 years of GADS data from the PJM Interconnection (PJM), the largest electric power market in the USA. For each generator, the two-state Markov model's time-varying probabilities are modeled as functions of exogenous variables using logistic regression. We model transition probabilities as a function of temperature and system load, though the model can be extended to include additional covariates. Both temperature and load vary with time and are jointly experienced by many generators, thus transition probabilities in generators' Markov chains can be correlated.

2. Model

We use logistic regression to model each generator's transition probabilities as a function of covariates. We fit these models using the GLM library in R, with default initial values. While there are many binary classification algorithms, logistic regression is relatively insensitive to unbalanced data [33]. This is an important attribute for this analysis, as most generators fail infrequently. Unbalanced data makes accurately estimating transition probabilities more difficult [34].

We employ a two-state Markov model wherein each generator is treated as either fully available (subsequently referred to as available and abbreviated A) or at least partially unavailable (subsequently referred to as derated and abbreviated D). For each generator we separately model two pairs of transition probabilities: the probability of an available generator remaining available in the next hour versus becoming derated (failing), and the probability of a derated generator remaining derated in the next hour versus becoming available (recovering).

As in [32], we allow transition probabilities to be a function of covariates. We consider temperature and load because they have time series dependence and affect multiple generators simultaneously. As a result, if they are found to have statistically significant associations with changes in transition probabilities, our model may be able to explain the correlated failures identified in [8]. If no covariates are statistically significant, this model reduces to the familiar homogeneous (time-invariant) Markov model of [11] (Fig. 1). Our modeling approach therefore allows us to relax the assumptions of unconditional independence and constant generator availability where empirically warranted. It instead assumes that generator transitions are

conditionally independent (after conditioning on relevant covariates) and allows generator availability to vary over time.

We fit our models using maximum likelihood estimation (iteratively reweighted least squares). Consistency and asymptotic normality of our coefficient estimates flow from traditional maximum likelihood estimation theory, which holds in our setting because all covariates are bounded [35]. The estimation procedure is conducted on each generator, using its hourly series of Markov state transitions and covariate data, described below. If the transition probabilities were constant, this would be equivalent to determining the probability of a coin coming up heads. The likelihood functions are:

$$\mathcal{L}(\beta_A) = \prod_{i=1}^{\text{count}(A)} Q_i(\beta_A)^{\alpha_i} * (1 - Q_i(\beta_A))^{1-\alpha_i} \quad (1)$$

$$\mathcal{L}(\beta_D) = \prod_{i=1}^{\text{count}(D)} P_i(\beta_D)^{\delta_i} * (1 - P_i(\beta_D))^{1-\delta_i} \quad (2)$$

where β_A and β_D are vectors of parameters for the available and derated models, respectively; Q_i is the probability of the generator remaining available in the next hour when it is currently available; P_i is the probability of the generator remaining derated in the next hour when it is currently derated; $\text{count}(A)$ is the number of observations used to fit the available model; $\text{count}(D)$ is the number of observations used to fit the derated model; $\alpha_i = 1$ if the i th available observation is AA and 0 otherwise; $\delta_i = 1$ if the i th derated observation is DD and 0 otherwise; and the sum of $\text{count}(A)$ and $\text{count}(D)$ equals the number of Markov state transitions in the reporting period for the generator. The available and derated models are fit separately for each generator (Fig. 2). A generator's hourly states are independent and identically distributed conditional on the covariate values; dependence in the covariate values leads to a richer time series structure for the generator's observations.

We allow Q_i and P_i to be functions of covariates while still ensuring all transition probabilities are bounded by [0,1] by employing the logistic function:

$$Q_i(\beta_A) = 1/(1 + \exp(-\beta_A X_i)) \quad (3)$$

$$P_i(\beta_D) = 1/(1 + \exp(-\beta_D X_i)) \quad (4)$$

where X_i is a vector of covariate observations in hour i , with as many elements as the number of constants and covariates in the model.

We consider the following model specification for both available and derated models for each generator:

$$\begin{aligned} \text{Index}_i = & \beta_1 * \text{constant}_{\text{hot}_i} + \beta_2 * \text{constant}_{\text{cool}_i} + \beta_3 * \text{degrees}_{\text{hot}_i} + \beta_4 \\ & * (\text{degrees}_{\text{hot}_i})^2 + \beta_5 * \text{degrees}_{\text{cool}_i} + \beta_6 * (\text{degrees}_{\text{cool}_i})^2 + \beta_7 \\ & * \text{system_load}_i \end{aligned} \quad (5)$$

where $\beta X_i = \text{Index}_i$ (linking Eqs. (3)–(5)), d $\text{egrees}_{\text{hot}_i} = \max(\text{temperature}_i - 18.3, 0)$, $\text{degrees}_{\text{cool}_i} = \max(18.3 - \text{temperature}_i, 0)$, system_load_i is the load residual in hour i , $\text{constant}_{\text{hot}_i} = 1$ if $\text{temperature}_{\text{cool}_i} = 0$ (and 0 otherwise), $\text{constant}_{\text{cool}_i} = 1$ if $\text{temperature}_{\text{cool}_i} > 0$ (and 0 otherwise), and temperature_i is the temperature in hour i , reported in degrees Celsius.² This specification allows for an asymmetric response to hot and cold temperature.

So that our model can better generalize to temperatures and loads not observed in the data, we employ stepwise regression (backward elimination) as described in Procedure 1, selecting a significance

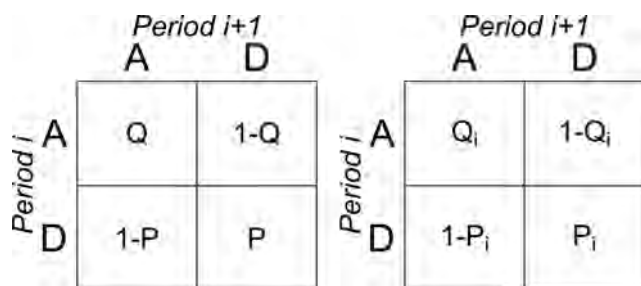


Fig. 1. Homogeneous (left) and nonhomogeneous (right) two-state Markov models. A indicates the available state, D indicates the derated state. Q and Q_i are the constant and time-varying probabilities of an AA transition, respectively. P and P_i are the constant and time-varying probabilities of a DD transition, respectively.

² 18.3 degrees Celsius is approximately 65 degrees Fahrenheit. This corresponds to the demarcation point used to define heating degree days and cooling degree days in the USA by the National Oceanic and Atmospheric Administration [49]. It also corresponds to the flattest region of the temperature-load relationship in the PJM area found by [50].

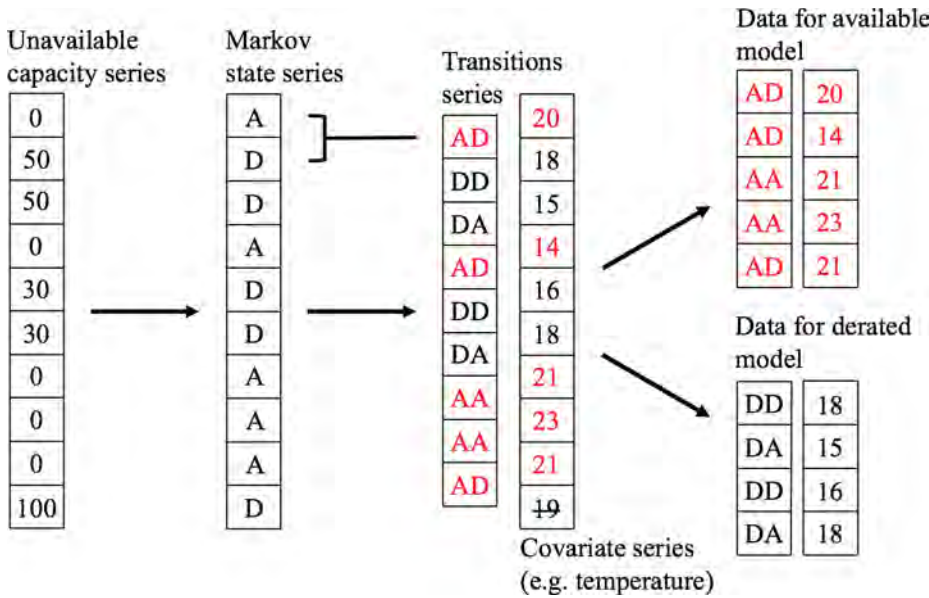


Fig. 2. Defining a generator's time series of transitions and allocating them to the available and derated models. The generator's hourly time series of unavailable capacity is first used to determine which Markov state the generator is in in each hour. The series of hour-over-hour state transitions is then determined. These observations, along with our covariates (illustrated as a single vector of hourly temperatures for clarity of presentation) are then allocated to the available and derated models. Any observation in which a generator begins in the A state is assigned to the available model, whereas any observation in which a generator begins in the D state is assigned to the derated model. Note that there are one fewer transitions than original observations, so the final covariate observation is not used.

level of 0.05. To reduce bias, we then eliminate any generator having fewer than 10 DA or AD transitions per statistically significant model covariate [36].³

Procedure 1 (Adaptive logistic regression model fitting).

- For each generator, do:
 - For each model (i.e., available and derated), do:
 - Fit full model specification (Eq. (5))
 - While model has one or more linearly dependent or statistically insignificant covariates, do:
 - If model has one or more linearly dependent covariates, remove one linearly dependent covariate and re-estimate model
 - Else, remove covariate with smallest t-value magnitude and re-estimate model
 - Save final model
- Remove generators that do not have at least 10 AD and 10 DA transitions per final model parameter

2.1. Simulating unavailable capacity from nonhomogeneous Markov models

Procedure 2 simulates time series of unavailable capacity for each generator according to the hourly failure and recovery probability distributions defined by the historical series of covariate values. Any hour that was ignored when fitting a generator's available or derated model is set to zero in both the empirical and simulated series. In order to have a true out-of-sample test of model performance, we refit the models using only 1995–2015 data (rather than 1995–2018) and retain just the 1047 generators that have sufficient transitions over the shortened time series. This leaves 2016–2018 as test data. We carry out this procedure 5000 times and generate pointwise median and 95% confidence intervals from the result, which we plot along with the empirical time series (Fig. 4). Given the data limitations discussed in Section 3.2.4, we repeat the process fitting only on 2004–2015 data, again leaving 2016–2018 as test data (Supplementary materials Fig. B.1⁴). For reference, we report annual installed capacity values for these generators (Table A.1 and Table B.1).

³ DA or AD is always the least-experienced transition.
⁴ Appendix A (with figures and tables numbered A.1, A.2, etc.) and Appendix B (with figures and tables numbered B.1, B.2, etc.) may be found in the supplementary materials, available online at <https://doi.org/10.1016/j.apenergy.2019.113513>.

Procedure 2 (Simulating unavailable capacity from nonhomogeneous Markov models).

- For each simulation, do:
 - For each generator, do:
 - Initialize the state of the generator to match its reported state during its first hour of data reporting
 - For each subsequent hour of the generator's reporting period, do:
 - Use the current state of the generator and the current values of all model covariates to define the current transition probability distribution (AA/AD if currently available; DD/DA if currently derated)
 - Draw 0 or 1 using the probability distribution defined above, where 0 indicates the generator is available and 1 indicates the generator is derated
 - Replace all 1s with the generator's average unscheduled capacity reduction to yield a time series of unscheduled unavailable capacity
 - Zero out any unavailable capacity occurring during hours removed during model fitting
 - Sum over generators' time series to obtain one simulated system-level time series
- Compute desired quantiles from simulation results (e.g. 2.5%, 50%, 97.5%) and save

2.2. Simulating unavailable capacity from time-invariant (homogeneous) Markov models per current RAM practice

We compute the equivalent forced outage factor (EFOF⁵), a common availability statistic, as follows [37]:

$$EFOF = (FOH + EFDH)/PH \tag{6}$$

where FOH (forced outage hours) is the sum of hours where the generator experiences a forced outage, EFDH (equivalent forced derating hours) is the sum of hours where the generator experiences a forced derating, reported in full-outage-equivalent hours, and PH (period hours) is the total number of hours in the period of interest. In accord with current RAM practice, we define the period supporting each planning year as the preceding five calendar years. For consistency with

⁵ More commonly, the equivalent forced outage rate (EFOR) is used [37]. $EFOR = (FOH + EFDH)/(FOH + SH + Synch + Pump + EFDHRS)$, where SH (service hours) is the total number of hours the generator produces electricity, Synch is the number of hours the generator operates in synchronous condensing mode, Pump is the number of hours a pumped-storage hydroelectric generator operates in pumping mode, and EFDHRS (equivalent forced derating hours during reserve shutdown) is the number of hours the generator experiences a forced derating during a reserve shutdown event, reported in full-outage-equivalent hours [39]. However, using EFOF allows us to not worry about incomplete reporting of reserve shutdown events prior to 2004.

the logistic regression results, we carry out the procedure for the 1047 generators retained when fitting models on 1995–2015 data and we ignore contributions to FOH and EFDH that occur during any hour removed during model fitting.

Procedure 3 (Simulating unavailable capacity from homogeneous Markov models).

Define duration of data period supporting each planning year (e.g. 5 years) For each simulation, do:

- For each planning year (e.g. 2000–2018), do:
 - For each generator, do:
 - If the generator was active during period supporting planning year and does not retire prior to planning year, do:
 - Compute EFOF (Eq. (6)) using all of generator's data supporting current planning year, except for hours removed during model fitting
 - For each hour in planning year, draw a 1 with probability equal to generator's EFOF and 0 otherwise, where 0 indicates the generator is available and 1 indicates the generator is unavailable
 - Replace all 1s with the generator's nameplate capacity
 - Sum over generators' time series to get one simulated system-level series for current planning year

Compute desired quantiles from simulation results (e.g. 2.5%, 50%, 97.5%) and save

2.3. Characterizing unavailable capacity as a function of temperature

Procedure 4 (Characterizing unavailable capacity as a function of temperature).

For each desired quantile of load (e.g. 50th, 90th), do:

- For each desired temperature value (e.g. spanning the range of temperatures experienced by the fleet, in 5-degree intervals), do:
 - Fix the value of temperature
 - Fix the value of load at the current load quantile, calculated on observations in the "neighborhood" of the current temperature value (e.g. within ± 10 degrees)
 - For each generator, do:
 - Compute predicted transition probabilities using generator's available and derated model and current temperature and load values
 - Define transition probability matrix as the transpose of Fig. 1
 - Normalize the first eigenvector of the eigendecomposition of the transition probability matrix to obtain the proportion of the time the generator is unavailable in expectation
 - Multiply result by generator's nameplate capacity and its average unscheduled capacity reduction to obtain expected unavailable capacity
 - Sum expected unavailable capacity values over generators and save

3. Data

3.1. GADS data description

The GADS database records availability and design information for all generators serving the PJM control area, with the exception of wind, solar, and behind-the-meter generation. Reporting to GADS is mandatory, regardless of generator size [38]. We work primarily with the Events, Units, and Performance tables. The Events table reports any event affecting the ability of a generator to produce electricity, as well as other event types defined by the Institute of Electrical and Electronics Engineers (IEEE) Standard 762 [37]. The Units table reports design details of each generator, such as generator type and nameplate capacity.⁶ The Performance table reports monthly summary statistics of each generator's operating and non-operating time. We analyze data from January 1, 1995 (database inception) through March 31, 2018. Over this period 1845 generators representing 267 GW (GW) of

⁶ The generator types include combined cycle gas (abbreviated as CC in figures and tables), simple cycle gas (CT), diesel (DS), hydroelectric and pumped storage (HD), nuclear (NU), and steam turbine (ST). In 2017, the vast majority (95%) of ST generation in PJM was from coal, thus we use the two terms interchangeably [48].

capacity have reported to GADS.

3.2. GADS data processing

3.2.1. Obtaining time series of availability state transitions

PJM's GADS database is virtually identical to that of NERC (albeit covering many more years), thus we prepare it for analysis as described in [8]. We calculate the magnitude of each derating event and then process events into time series of unavailable capacity. We restrict each generator's time series to complete calendar years. We then use each generator's time series of unavailable capacity to define a corresponding time series of hour-over-hour Markov state transitions (Fig. 2). For example, an AA transition occurs when the generator is available in two adjacent hours.

3.2.2. Determining when a generator is available to transition

Our model assumes each generator is able to transition out of its current state in each hour (i.e., the generator can experience a failure if it is currently available and recover if currently derated). We attempt to exclude hours in which this assumption is violated in order to minimize bias. When fitting the available model, we remove mothball, inactive reserve, and all scheduled outage events because the generator cannot be operating when these events are underway [39]. The generator can still operate when a scheduled derating is in effect, so these hours are not removed.

When fitting the derated model, we remove only mothball and inactive reserve events. This is because no repair work is allowed to occur when these events are in progress [39]. Repair work on unscheduled failures can occur during scheduled outage and scheduled derating events, so these hours are not removed. In addition, some failures are catastrophic and take many months to repair. Including these events would bias recovery probabilities downward. To correct for this, we remove hours when a generator remains in the derated state without interruption for more than six months.

3.2.3. Calculating the average derating magnitude for each generator

Because derating magnitudes can take any value up to a generator's nameplate capacity, but our model allows only one derated state, we calculate the average failure magnitude for each generator (Fig. A.1). We calculate this as a duration-weighted average of all unscheduled events experienced by the generator, excluding any hour removed when fitting either the available or derated model. The average and median failure magnitudes are 78% and 96% of nameplate capacity, respectively.

3.2.4. A note on reserve shutdown events

Reserve shutdown events are used to indicate when a generator is offline for economic reasons but is capable of coming online within its normal startup time if needed. With the exception of hydroelectric and pumped storage generators without automatic reporting equipment, all conventional generators participating in the PJM market became obligated to report reserve shutdown events to GADS in January 2004, nine years after the beginning of our data.

When a reserve shutdown event is underway, a generator should neither be in service nor have repair work conducted. If one assumes that the incidence of a failure while a generator is not operating and not being repaired is much lower than when operating or when being repaired, reserve shutdown hours should also be excluded from both available and derated model fits. However, given that most generators fail infrequently and that we require a minimum of 10 AD and DA transitions per statistically significant covariate to keep a generator in our analysis, eliminating the first nine years of data results in significantly fewer generators retained, particularly for CTs.

As a result, we fit our models twice: first using the full data period (1995–2018) ignoring reserve shutdown events, and second restricting to 2004–2018 and removing reserve shutdown hours from both

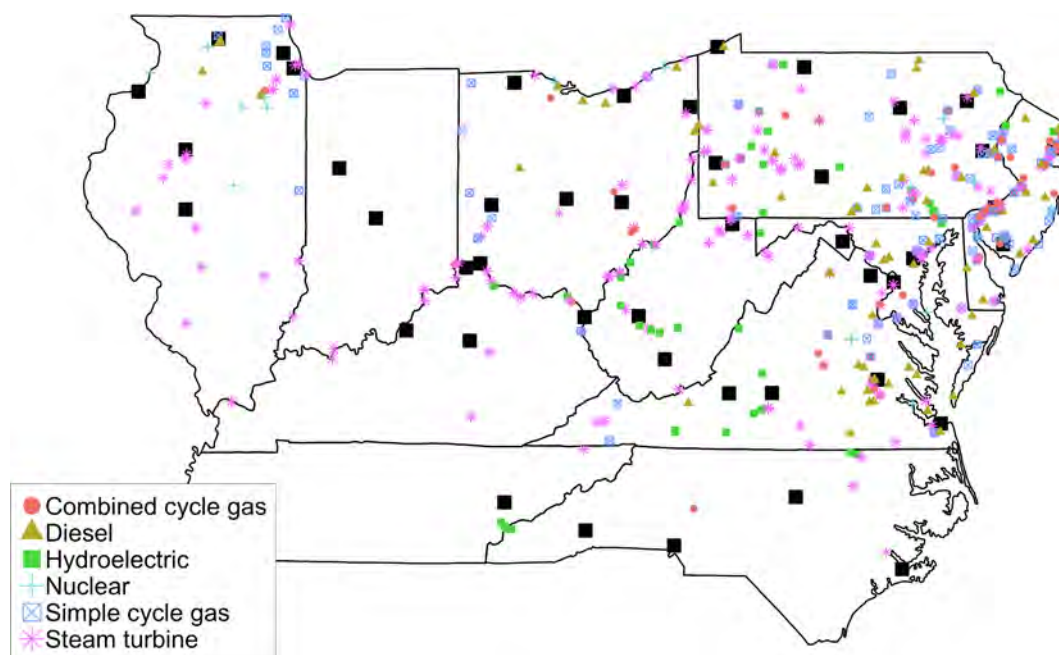


Fig. 3. Locations of 1111 retained generators and linked weather stations, overlaid on corresponding USA states (1995–2018 model fits). Only generators with at least 10 failure and recovery transitions per statistically significant model parameter are retained. All generators in multi-generator power plants have identical locations. Large black squares indicate weather stations. A small number of retained generators are not shown for presentation considerations: Alabama (3), Louisiana (5), Michigan (23), Mississippi (3), South Carolina (1), Texas (8).

available and derated model fits. Results based upon the former are presented in the main text and in Appendix A, while results based upon the latter are included in Appendix B. In general, we find reasonable agreement between the two sets of results.

3.3. Geographic, weather, and load data processing

3.3.1. Geocoding generators

To determine the location of each generator, we match the GADS data to the Emissions and Generation Resource Integrated Database (eGRID), maintained by the USA Environmental Protection Agency [40–43]. This task was completed using a combination of automated and manual matching using generator names and other descriptive fields. We manually confirm each automated match and then associate the eGRID latitude/longitude data with the generator.

3.3.2. Weather station data

We obtain temperature data from the Global Surface Hourly database, maintained by the USA National Oceanic and Atmospheric Administration [44]. We include all weather stations active for the full study period in any state containing or adjacent to any generator. We process these data into hourly time series for each weather station by first rounding observations to the nearest hour and then removing observations with duplicate time stamps. We discard any weather station missing more than 100 sequential observations or more than 5000 total observations over the 23 years, with three exceptions to increase coverage in Pennsylvania.⁷ We then fill missing observations by propagating forward the most recent non-missing observation.⁸ Finally, we link each generator to its nearest weather station meeting our data criteria. We map the retained generators and matched weather stations

⁷ These three stations had 268, 65, and 103 sequential missing observations and 2937, 8962, and 1370 total missing observations.

⁸ We initially filled missing observations by propagating forward the most recent non-missing observation at the same hour of the day, but discovered that several weather stations were systematically missing observations at particular times of the day over long durations.

(Fig. 3 and Fig. B.2).

3.3.3. Load data

Finally we obtain hourly metered load data by PJM transmission zone for the full study period. We sum over all zones that have been part of the control area since January 1995 to develop an hourly load series for the system.⁹ To account for non-stationarities in that series, we regress the load data on a constant, a linear time trend, and a quadratic time trend. The residuals from this linear regression are used as the load signal experienced by each generator. We plot the load time series with regression trend and residuals (Fig. A.2 and Fig. B.3).

3.4. Model significance summaries

When fitting models on the full dataset, we retain 1111 of 1845 generators, representing 78% of the capacity that has ever reported to GADS (Fig. A.3); when restricting to 2004–2018, we retain 748 generators representing 67% of capacity (Fig. B.4). While failures and recoveries for the remaining generators may indeed be influenced by temperature and/or load, they have so few transitions that we would not have confidence in the fitted models. We summarize the count and capacity of these generators (Table A.2 and Table B.2).

We summarize marginal statistical significance of the covariates by plotting parameter t-values by generator type (Figs. A.4–A.5 and Figs. B.5–B.6) and reporting the number of times each model term is statistically significant at the 95% level by generator type (Tables 1, 2 and Tables B.3–B.4). We include corresponding summaries of model coefficients (Figs. A.6–A.7 and Figs. B.7–B.8).

When fitting on the full dataset, linear and quadratic hot-temperature variables are statistically significant for 19% and 17% of

⁹ We include: Allegheny Power, Atlantic City Electric Company, Baltimore Gas and Electric Company, Delmarva Power and Light Company, Jersey Central Power and Light Company, Metropolitan Edison Company, PPL Electric Utilities Corporation, Pennsylvania Electric Company, Philadelphia Electric Company, Potomac Electric Power Company, and UGI.

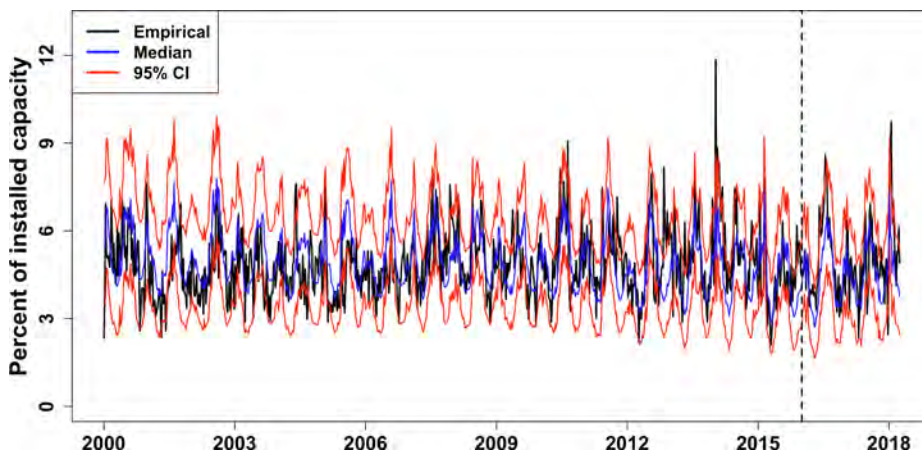


Fig. 4. Simulated time series from logistic regression model (1995–2015 model fits). Results presented for 1047 generators with at least 10 failure and recovery transitions per statistically significant model parameter when fitting on 1995–2015; 2016–2018 used as test of model performance. The split between training and testing periods is denoted with a dashed vertical line. Presented for 2000–2018 for consistency with Fig. 5. Weekly averages rather than hourly series. 5000 simulations conducted. Refer to Table A.1 for installed capacity by calendar year. Black trace is the empirical time series; blue trace is the concatenation of pointwise median simulation values; red traces are the concatenation of pointwise 2.5% and 97.5% simulation values.

Table 1

Number of times each model term is statistically significant at the 95% level for the available model (1995–2018 model fits). Only generators with at least 10 failure and recovery transitions per statistically significant model parameter are retained. CC is combined cycle, CT is simple cycle, DS is diesel, HD is hydroelectric and pumped storage, NU is nuclear, ST is steam turbine.

Generator type	Generator count	Mean hot	Mean cool	Temp hot	Temp hot ²	Temp cool	Temp cool ²	Load
CC	148	148	148	25	26	75	115	41
CT	274	274	274	59	53	110	203	228
DS	132	131	132	32	30	59	29	104
HD	125	125	125	16	14	22	35	43
NU	35	35	35	10	10	9	7	15
ST	397	397	397	70	61	103	134	285
All	1111	1110	1111	212	194	378	523	716

generators' available models; linear and quadratic cold-temperature variables are statistically significant for 34% and 47% of generators' available models; and load is statistically significant for 64% of generators' available models. For the derated model, linear and quadratic hot-temperature variables are statistically significant for 23% and 20% of generators; linear and quadratic cold-temperature variables are statistically significant for 36% and 35% of generators; and load is statistically significant for 68% of generators.

We summarize the joint statistical significance of model covariates by creating scatterplots of parameter t-values between all non-orthogonal covariate pairs, excluding constants (Figs. A.8–A.9 and Figs. B.9–B.10).¹⁰ We observe systematic joint statistical significance between linear and quadratic temperature parameters in both sets of models, suggesting true temperature dependence rather than individual temperature parameters being significant by random chance. We include corresponding bivariate summaries of model coefficients (Figs. A.10–A.11 and Figs. B.11–B.12).

We report the number of statistically significant parameters for each generator (Table A.3 and Table B.5). We report similar information when restricting attention to linear and quadratic temperature parameters (Table A.4 and Table B.6). When fitting on the full dataset, 69% of generators have at least one statistically significant temperature covariate for the available model; 67% do for the derated model. These results demonstrate that temperature and load can have independent effects on transition probabilities. Finally, we compactly summarize variation in model predictions over the experienced covariate observations for each generator (Supplementary materials Fig. A.12 and Fig. B.13).

¹⁰ Recall that hot-temperature covariates are defined orthogonal to cool-temperature covariates.

4. Results

In the previous section, we demonstrate that temperature and load can predict state transitions at the generator level. We use Monte Carlo simulation to demonstrate that the models can also predict correlated failures (Procedure 2). Even with our simple model specification using only temperature and load as covariates, we find that the median simulation generally tracks the empirical time series quite well (Fig. 4 and Fig B.1). The correlation between weekly average median simulation values and weekly average empirical values is 0.47 and 0.67 over the training and testing periods, respectively, for the 1995–2015 model fits and 0.47 and 0.69 during training and testing periods for the 2004–2015 fits. The motivation for fitting models using two different time periods is explained in the previous section.

Furthermore, it is rare for an empirical event to exceed the upper confidence band of our model. The largest instances of under-prediction by our model occurred during two known events in which significant generator outages were due to causes not included as covariates: the 2014 Polar Vortex (due to fuel unavailability events, which increase non-linearly in cold weather) and Hurricane Sandy (an extreme weather event but not with regard to temperature). While many other factors may contribute to generator failures and recoveries [45–47], these results demonstrate that temperature and load are strongly correlated with system-level unavailable capacity dynamics.

We next compare the performance of our model to that of current RAM practice. This entails computing an availability statistic for each generator in each planning year (Eq. (6)), and then using those statistics in Monte Carlo simulations (Procedure 3).

We plot the pointwise median and 95% confidence intervals from 5000 simulations of the current RAM practice (Fig. 5). As anticipated, the current practice approach does not capture correlated failures because the distribution of unavailable capacity is the same in every hour of a given planning year. The correlation between weekly average median simulation values and weekly average empirical values is 0.15

Table 2

Number of times each model term is statistically significant at the 95% level for the derated model (1995–2018 model fits). Only generators with at least 10 failure and recovery transitions per statistically significant model parameter are retained. CC is combined cycle, CT is simple cycle, DS is diesel, HD is hydroelectric and pumped storage, NU is nuclear, ST is steam turbine.

Generator type	Generator count	Mean hot	Mean cool	Temp hot	Temp hot ²	Temp cool	Temp cool ²	Load
CC	148	147	148	38	35	61	52	100
CT	274	270	272	65	54	104	124	242
DS	132	131	130	40	31	56	67	113
HD	125	124	124	24	16	39	41	93
NU	35	35	35	13	11	12	6	10
ST	397	397	397	73	79	125	101	192
All	1111	1104	1106	253	226	397	391	750

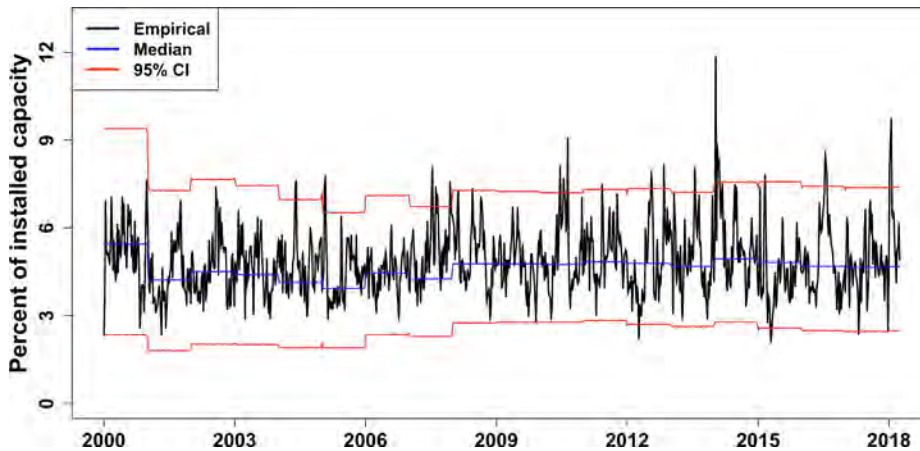


Fig. 5. Simulated time series from current practice model (1995–2015 model fits). Results presented for the same set of 1047 generators as in Fig. 4. Time series restricted to 2000–2018 because five years of data are used to calculate the availability statistic (Eq. (6)). Traces are flat within each calendar year because current practice model assumes failure probabilities are constant in each hour of a given year. Small discontinuities at year boundaries are due to weekly averaging not respecting calendar year boundaries, in conjunction with capacity additions and retirements occurring at the start of the year. Weekly averages rather than hourly series. 5000 simulations conducted. Refer to Table A.1 for installed capacity by calendar year. Black trace is the empirical time series; blue trace is the concatenation of pointwise median simulation values; red traces are the concatenation of pointwise 2.5% and 97.5% simulation values.

over 18 years and 0.11 during the testing period.¹¹ In addition, the pointwise 95% confidence intervals are wider than those for our model, averaging 5% of installed capacity over 18 years compared to 3.1% of installed capacity for the logistic regression model.

Comparing the two figures, we observe that the homogeneous Markov model simulating current RAM practice would both under-procure reserve generation for ~ 10 events and over-procure reserves most of the time. That the nonhomogeneous model tracks observed failure dynamics substantially better than the current practice model suggests its potential utility both for improving the accuracy of RAM and for predicting correlated failures over time horizons relevant to procurement of operating reserves.

4.1. Resource adequacy risk as a function of temperature and load

We next examine resource adequacy risks for the fleet of generators in PJM. For fixed values of temperature and load, each generator's available and derated models imply a stationary distribution over the available and derated states. We make use of this fact to determine the proportion of the time each generator is unavailable in expectation. By calculating this result over a range of temperature values, we determine expected unavailable capacity as a function of temperature for the modeled fleet (Procedure 4). We determine the analogous result under current modeling practice by first computing an unconditional transition probability matrix for each generator using all available years of data and then following the remainder of the inner loop of Procedure 4. We present results by generator type (Fig. 6 and Fig. B.14) and report the prevalence of temperatures experienced by the fleet of modeled generators (Fig. A.13 and Fig. B.15).

With the exception of nuclear, all generator types perform worse in

very cold weather than recognized under current modeling practice. This result is consistent with analysis conducted by PJM [2]. Poor cold-weather performance is particularly pronounced for gas and diesel generators. In addition, all generator types perform worse in very hot weather than recognized under current practice. Because loads are high at both temperature extremes, the resource adequacy risk implied by these performance penalties is compounded: less generation capacity is available when demand is greatest. In power systems with organized forward-capacity markets, these temperature-dependent performance penalties could be used to improve capacity payments. Rather than use a generator's unconditional forced outage rate to determine capacity payments [48], thereby penalizing the generator for its average unavailability, the grid planner could calculate a conditional forced outage rate during relevant extreme weather conditions that represent increased resource adequacy risk.

Finally, we repeat the preceding analysis switching the role of temperature and load in order to visualize resource adequacy risk as a function of load. Because the relationship between load and unavailable capacity could be different at high and low temperatures, we generate two sets of results: one for observations where the temperature is below 18.3 degrees, and one for observations where temperature is above 18.3 degrees. With these modifications, we repeat Procedure 4. We again present results by generator type (Figs. A.14–A.15 and Figs. B.16–B.17).

In Fig. A.14, at median temperature values, only coal generators at very high loads show noticeable divergence from the unconditional level of unavailable capacity. When considering low-percentile temperatures, gas and diesel generators also exhibit divergence from the unconditional result at higher loads. Nuclear generators show no load response for cold-temperature observations, regardless of load level or temperature quantile, consistent with Fig. 6. In Fig. A.15, coal and nuclear generators diverge from their respective unconditional levels of unavailable capacity at high loads regardless of temperature percentile considered. Diesel generators show some divergence at very low loads.

¹¹ Note that the predictions of the current practice model are always out of sample, in contrast with those of the logistic regression model prior to 2016.

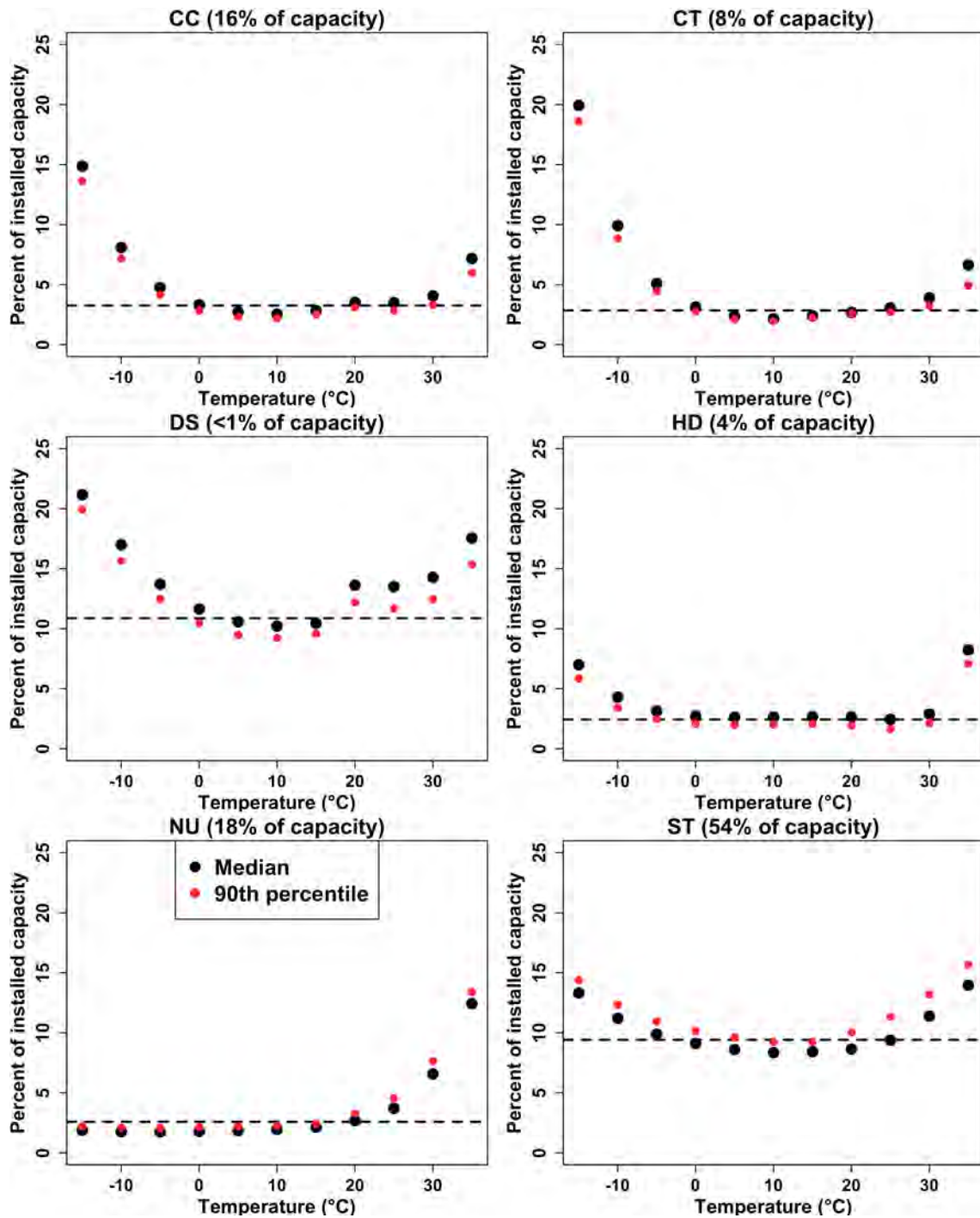


Fig. 6. Expected levels of unavailable capacity as a function of temperature under logistic regression (dots) and current practice (dashed horizontal line) (1995–2018 model fits). Black dots calculated using median load from temperature neighborhood, red dots calculated using 90th percentile load from temperature neighborhood. Temperature neighborhood is defined as ± 10 degrees. Not all generators experience full temperature range; see Fig. A.13 for prevalence of temperatures. CC is combined cycle, CT is simple cycle, DS is diesel, HD is hydroelectric and pumped storage, NU is nuclear, ST is steam turbine.

5. Discussion

We have presented a model of how correlated failures previously identified in the North American power system [8] can occur. Our approach is a novel, computationally tractable generalization of the traditional two-state Markov model widely used in power system reliability analyses [11]. We demonstrate a simple specification in which transition probabilities between the available and derated states are modeled as a function of temperature and load, but we note that any desired covariates could be employed.

We fit these models using logistic regression with 23 years of availability data for 1845 generators serving the PJM regional transmission organization. To reduce bias, we discard any generator with fewer than 10 failure or recovery events per statistically significant covariate. We retain 78% of the generation capacity that has ever reported to PJM GADS. We find that temperature and load can predict generator transitions: temperature and load are each statistically significant for two-thirds of the retained generators.

We demonstrate that our model specification captures most of the correlated failures observed in PJM since 2000 and that it significantly

outperforms the homogeneous Markov model underlying current resource adequacy modeling practice. The correlation of our median simulation with the observed series of unavailable capacity at the weekly level is 0.47 over 18 years, whereas that of the median simulation from current practice is 0.15. Our model also has narrower confidence intervals, averaging 3.1% of installed capacity compared to 5% for current practice.

6. Conclusions

We demonstrate that all generator types are susceptible to increased probability of failure at extreme temperatures. With the exception of nuclear generators, which have reduced availability during only hot weather, all generator types have reduced availability at both temperature extremes. The cold-weather penalty for gas and diesel generators is particularly pronounced, as is the hot-weather penalty for nuclear generators. These availability penalties, which represent temperature-dependent forced outage rates, could be used to determine capacity payments that better incentivize generators to be available during key times of grid stress. Finally, we demonstrate that nuclear and coal generators experience an availability penalty at high loads; for nuclear generators this penalty is present only in conjunction with high temperatures. These risks are not captured in current approaches to resource adequacy modeling.

Taken together, our results demonstrate that there are systematic relationships between temperature, load, and generator availability. Accounting for these relationships, as we have done here, is likely to enable more accurate determination of power system reserve capacity requirements. In particular, given that peak loads typically coincide with either very low or very high temperatures, the relationships we have identified suggest that current RAM practice may be underestimating power system reserve capacity requirements. Future work should examine the specific causes of the temperature dependence of generator availability and what improvements in reserves procurement can be achieved now that correlated failures can be successfully modeled.

Acknowledgements

This research was supported in part by the Carnegie Mellon Climate and Energy Decision Making Center (CEDM), formed through a cooperative agreement between the National Science Foundation and CMU (SES-0949710) and in part by the Electric Power Research Institute. No funding source had any role in study design, in analysis or interpretation of data, in the writing of the paper, or in the decision to submit it for publication. We are grateful to Tom Falin for access to the PJM GADS data. We thank Patricio Rocha-Garrido and Francis J. Bell III for many helpful discussions.

Declaration of Competing Interest

The authors declare no conflicts of interest.

Appendix A. Supplementary material

Supplementary data to this article can be found online at <https://doi.org/10.1016/j.apenergy.2019.113513>.

References

- [1] Gaver DP, Montmeat FE, Patton AD. Power system reliability I: Measures of reliability and methods of calculation. *IEEE Trans Power Appar Syst* 1964;83:727–37.
- [2] PJM. Problem statement on PJM Capacity Performance definition. 2014. < <https://www.pjm.com/-/media/library/reports-notices/capacity-performance/20140801-problem-statement-on-pjm-capacity-performance-definition.aspx?la=en> > .
- [3] PJM. PJM Cold Snap Performance: December 28, 2017 to January 7, 2018. 2018. < <https://www.pjm.com/-/media/library/reports-notices/weather-related/20180226-january-2018-cold-weather-event-report.aspx> > .
- [4] Billinton R, Allan RN. Reliability evaluation of power systems. 2nd ed. Plenum; 1996.
- [5] Fegan GR. Reliability calculations for interdependent plant outages. EPRI report EL-3669 1984.
- [6] Li W. Risk assessment of power systems: models, methods, and applications. 1st ed. IEEE Press; 2005.
- [7] Billinton R, Li W. Reliability assessment of electric power systems using Monte Carlo methods. 1st ed. Springer; 1994.
- [8] Murphy S, Apt J, Moura J, Sowell F. Resource adequacy risks to the bulk power system in North America. *Appl Energy* 2018;212:1360–76.
- [9] Spees K, Newell SA, Pfeifenberger JP. Capacity markets - Lessons learned from the first decade. *Econ Energy Environ Policy* 2013;2:1–26.
- [10] IEEE Probability Application for common mode events working group of the reliability risk and probability applications subcommittee. research on common-mode and dependent (CMD) outage events in power systems: a review. *IEEE Trans Power Syst* 2017;32:1528–36.
- [11] Billinton R, Allan RN. Reliability Evaluation of Engineering Systems. 2nd ed. Springer; 1992.
- [12] Lisnianski A, Laredo D, Benhaim H. Multi-state Markov model for reliability analysis of a combined cycle gas turbine power plant. *Second Int. Symp. Stoch. Model. Reliab. Eng. Life Sci. Oper. Manag.* 2016.
- [13] Billinton R, Bollinger KE. Transmission system reliability evaluation using Markov processes. *IEEE Trans Power Appar Syst* 1968;PAS-87:538–47.
- [14] Liu Y, Singh C. Evaluation of hurricane impact on composite power system reliability considering common-cause failures. *Int J Syst Assur Eng Manag* 2010;1:135–45. <https://doi.org/10.1007/s13198-010-0024-7>.
- [15] Billinton R, Li W. A novel method for incorporating weather effects in composite system adequacy evaluation. *IEEE Trans Power Syst* 1991;6:1154–60. <https://doi.org/10.1109/59.119260>.
- [16] Bhavaraju MP, Hynds JA, Nunan GA. A method for estimating equivalent forced outage rates of multistate peaking units. *IEEE Trans Power Appar Syst* 1978;2067–75.
- [17] Billinton R, Chowdhury AA. A model for peaking units using the Canadian Electrical Association data base. *IEEE Trans Power Appar Syst* 1985;PAS-104:2972–9.
- [18] IEEE Task Group on Models for Peaking Service of the Application of Probability Methods Subcommittee. A four-state model for estimation of outage risk for units in peaking service. *IEEE Trans Power Appar Syst* 1972;PAS-91:618–27.
- [19] Bramer LM, Rounds J, Burleyson CD, Fortin D, Hathaway J, Rice J, Kraucunas I. Evaluating penalized logistic regression models to predict heat-related electric grid stress days. *Appl Energy* 2017;205:1408–18.
- [20] Li G, Zhang P, Luh PB, Li W, Bie Z, Serna C, Zhao Z. Risk analysis for distribution systems in the northeast US under wind storms. *IEEE Trans Power Syst* 2014;29:889–98.
- [21] Bernstein A, Bienstock D, Hay D, Uzunoglu M, Zussman G. Power grid vulnerability to geographically correlated failures – analysis and control implications. *IEEE INFOCOM 2014 - IEEE Conf Comput Commun* 2014.
- [22] Panteli M, Mancarella P. Modeling and evaluating the resilience of critical electrical power infrastructure to extreme weather events. *IEEE Syst J* 2017;11:1733–42.
- [23] Wei Y, Ji C, Galvan F, Couvillon S, Orellana G, Momoh J. Non-stationary random process for large-scale failure and recovery of power distribution. *Appl Math* 2016:233–49.
- [24] Liu Y, Trivedi KS. A general framework for network survivability quantification. *12th GI/ITG Conf Meas Model Eval Comput Commun Syst* 2005:1–10.
- [25] IEEE Probability Application for Common Mode Events Working Group of the Reliability Risk and Probability Applications Subcommittee. Overview of common mode outages in power systems. *IEEE Power Energy Soc. Gen. Meet. San Diego, California, USA, 2012*, p. 1–8.
- [26] Li W, Billinton R. Common cause outage models in power system reliability evaluation. *IEEE Trans Power Syst* 2003;18:966–8.
- [27] Billinton R. Basic models and methodologies for common mode and dependent transmission outage events. *IEEE Power Energy Soc Gen Meet* 2012:1–8.
- [28] Felder FA. Top-down composite modeling of bulk power systems. *IEEE Trans Power Syst* 2005;20:1655–6.
- [29] Hou K, Jia H, Xu X, Liu Z, Jiang Y. A continuous time Markov chain based sequential analytical approach for composite power system reliability assessment. *IEEE Trans Power Syst* 2016;31:738–48.
- [30] Andreasson M, Amin S, Schwartz G, Johansson K, Sandberg H, Sastry S. Correlated failures of power systems: analysis of the nordic grid. *Work Found Dependable Secur Cyber-Physical Syst CPSWeek 2011* 2011:9–17.
- [31] Wang J, Xiong X, Zhou N, Li Z, Weng S. Time-varying failure rate simulation model of transmission lines and its application in power system risk assessment considering seasonal alternating meteorological disasters. *IET Gener Transm Distrib* 2016;10:1582–8.
- [32] Ertekin S, Rudin C, McCormick TH. Reactive point processes: A new approach to predicting power failures in underground electrical systems. *Ann Appl Stat* 2015;9:122–44.
- [33] Crone SF, Finlay S. Instance sampling in credit scoring: An empirical study of sample size and balancing. *Int J Forecast* 2012;28:224–38.
- [34] King G, Zeng L. Logistic Regression in Rare Events Data. *Polit Anal* 2001;9:137–63.
- [35] Severini TA. Likelihood Methods in Statistics. Oxford University Press; 2000.
- [36] Peduzzi P, Concato J, Kemper E, Holford TR, Feinstein AR. A simulation study of the number of events per variable in logistic regression analysis. *J Clin Epidemiol* 1996;49:1373–9.
- [37] IEEE Power Engineering Society. Standard 762-2006: Standard definitions for use in reporting electric generating unit reliability, availability, and productivity. New

- York, NY: 2007.
- [38] Integ Enterprise Consulting. PowerGADS 3.0 User Manual. 2015. < <https://www.pjm.com/~media/etools/egads/egads-user-guide.ashx> > .
- [39] North American Electric Reliability Corporation. Generating Availability Data System: Data reporting instructions. 2018. < [https://www.nerc.com/pa/RAPA/gads/DataReportingInstructions/2018 GADS Data Reporting Instructions.pdf](https://www.nerc.com/pa/RAPA/gads/DataReportingInstructions/2018%20GADS%20Data%20Reporting%20Instructions.pdf) > .
- [40] United States Environmental Protection Agency. Emissions & Generation Resource Integrated Database (eGRID) 1996. (accessed September 3, 2017). < <https://www.epa.gov/energy/emissions-generation-resource-integrated-database-egrid> > .
- [41] United States Environmental Protection Agency. Emissions & Generation Resource Integrated Database (eGRID) 2000. (accessed September 3, 2017). < <https://www.epa.gov/energy/emissions-generation-resource-integrated-database-egrid> > .
- [42] United States Environmental Protection Agency. Emissions & Generation Resource Integrated Database (eGRID) 2014. (accessed September 3, 2017). < <https://www.epa.gov/energy/emissions-generation-resource-integrated-database-egrid> > .
- [43] United States Environmental Protection Agency. Emissions & Generation Resource Integrated Database (eGRID) 2016. (accessed July 24, 2018). < <https://www.epa.gov/energy/emissions-generation-resource-integrated-database-egrid> > .
- [44] NOAA National Centers for Environmental Information. Global Surface Hourly (DS3505) 2001. (accessed May 28, 2018). < <https://www7.ncdc.noaa.gov/CDO/cdopomain.cmd?datasetabv=DS3505&countryabv=&georegionabv=&resolution=40> > .
- [45] North American Electric Reliability Council. Predicting unit availability: Top-down analyses for predicting electric generating unit availability. 1991. < <https://www.nerc.com/pa/RAPA/gads/Publications/Predicting-Unit-Availability.pdf> > .
- [46] North American Electric Reliability Council. Seasonal performance trends: Peak season equivalent forced outage rate trend evaluations for fossil-steam generating units. 1991. < <https://www.nerc.com/pa/RAPA/gads/Publications/Seasonal-Performance-Trends.pdf> > .
- [47] North American Electric Reliability Council. Predicting generating unit reliability: A methodology for predicting generating unit reliability based on design characteristics, operational factors, and maintenance and plant betterment activities. 1995. < <https://www.nerc.com/pa/RAPA/gads/Publications/Predicting-Generating-Unit-Reliability.pdf> > .
- [48] Monitoring Analytics. 2017 State of the Market Report for PJM. vol. 2. 2018. < https://www.monitoringanalytics.com/reports/PJM_State_of_the_Market/2017.shtml > .
- [49] National Oceanic and Atmospheric Administration. National weather service glossary 2009. (accessed April 25, 2019). < <https://w1.weather.gov/glossary/index.php> > .
- [50] Lueken R, Apt J, Sowell F. Robust resource adequacy planning in the face of coal retirements. *Energy Policy* 2016;88:371–88.

Supplementary Materials:
A time-dependent model of generator failures and recoveries
captures correlated events and quantifies temperature dependence

Sinnott Murphy^a, Fallaw Sowell^b, Jay Apt^{a,b,*}

^a*Department of Engineering & Public Policy, Carnegie Mellon University, Pittsburgh, PA 15213*

^b*Tepper School of Business, Carnegie Mellon University, Pittsburgh, PA 15213*

36 pages, 32 figures, 10 tables

Contents

Appendix A: Figures and tables for 1995-2018 model fits	2
Appendix B: Figures and tables for 2004-2018 model fits	18

*e-mail: apt@cmu.edu (J. Apt)

Appendix A: Figures and tables for 1995-2018 model fits

Year	CC	CT	DS	HD	NU	ST	All
2000	4.2	7.1	0.1	3.3	19.5	69.2	103.5
2001	5.2	8.0	0.1	6.4	32.7	79.4	131.8
2002	6.3	9.8	0.1	6.4	32.7	80.4	135.7
2003	9.1	10.2	0.1	6.5	32.7	83.0	141.5
2004	15.6	11.1	0.1	7.2	34.9	83.8	152.9
2005	20.3	12.9	0.1	6.3	36.3	96.5	172.4
2006	21.2	12.9	0.2	5.9	36.3	96.6	173.1
2007	23.1	13.2	0.2	5.9	36.3	103.8	182.5
2008	24.9	13.4	0.3	6.0	36.3	103.3	184.1
2009	26.0	13.5	0.3	6.0	36.3	102.9	184.9
2010	25.8	13.6	0.3	6.0	36.3	103.1	185.1
2011	25.8	13.6	0.3	6.1	36.3	103.0	185.1
2012	28.1	13.3	0.4	6.1	36.3	95.7	179.8
2013	28.3	13.6	0.4	6.1	36.3	95.7	180.3
2014	29.1	13.0	0.4	6.1	36.3	94.0	178.9
2015	29.1	11.4	0.4	6.1	36.3	86.2	169.5
2016	29.1	10.9	0.4	6.1	36.3	85.2	167.9
2017	28.5	10.8	0.4	6.1	36.3	83.1	165.0
2018	28.5	10.8	0.4	6.1	36.3	82.9	164.9

Table A.1: Installed capacity (GW) of 1,047 retained generators by year and generator type (1995-2015 model fits). For use in conjunction with Figure 4 and Figure 5. CC is combined cycle, CT is simple cycle, DS is diesel, HD is hydroelectric and pumped storage, NU is nuclear, ST is steam turbine.

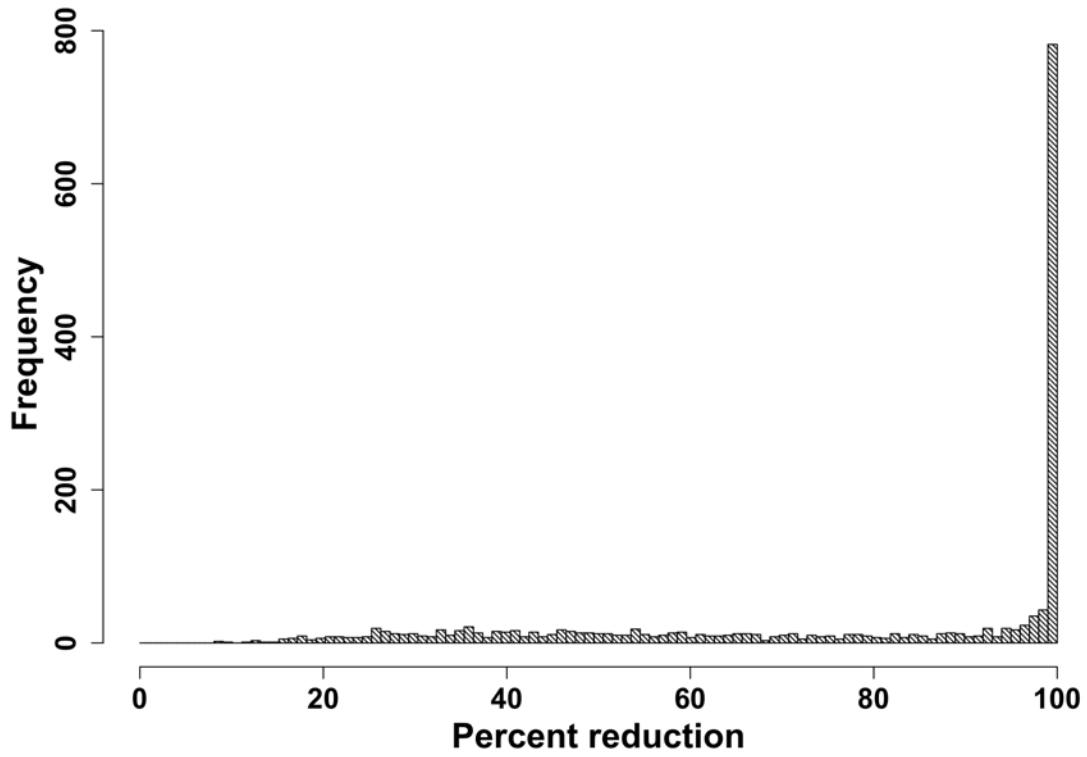


Figure A.1: Histogram of average generator failure magnitudes. Calculated for the 1,748 generators with at least one full calendar year of data reporting and at least one unscheduled transition during 1995-2018. Values calculated as a duration-weighted average of the magnitudes all unscheduled events experienced by the generator, excluding any hour removed when fitting either the available or derated model.

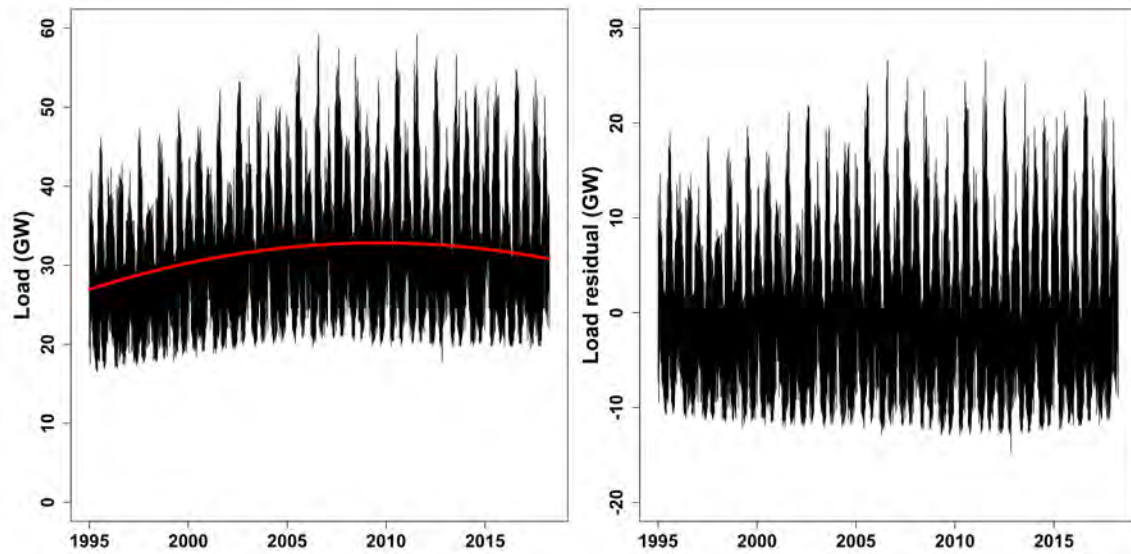


Figure A.2: Metered load time series (1995-2018 model fits). Left: hourly time series of metered system load for PJM transmission zones that have been part of PJM since database inception, with time trend (red curve) as described in Section 3.3.3. Right: residuals from fitting time trend to the original series.

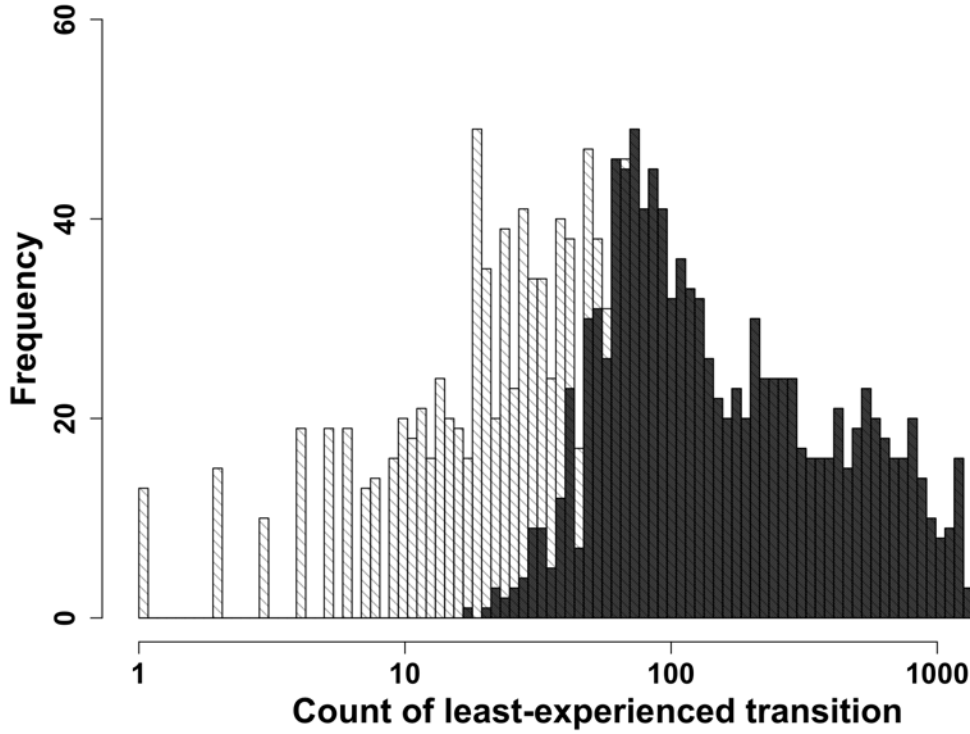


Figure A.3: Histogram of the count of least frequently experienced transition by generator (1995-2018 model fits). The 1,748 generators with at least one full calendar year of data reporting and at least one unscheduled transition during 1995-2018 are plotted in light gray. Of these, the 1,111 generators with at least 10 failure and recovery transitions per statistically significant parameter are then overplotted in dark gray. Above 70 such transitions the full model specification (Equation 5) can be supported, so no generators in corresponding bins are discarded. Note the log scale on the abscissa.

Generator type	Total count	Retained count (%)	Total capacity	Retained capacity (%)
CC	224	148 (66)	53.4	33.5 (63)
CT	663	274 (41)	44.9	16.5 (37)
DS	236	132 (56)	0.8	0.5 (58)
HD	244	125 (51)	11.0	8.3 (75)
NU	35	35 (100)	37.2	37.2 (100)
ST	443	397 (90)	119.5	113.1 (95)
All	1,845	1,111 (60)	266.8	209.0 (78)

Table A.2: Summary of total and retained generator counts and capacity, by generator type (1995-2018 model fits). Only generators with at least 10 failure and recovery transitions per statistically significant model parameter are retained. Capacity reported in GW. CC is combined cycle, CT is simple cycle, DS is diesel, HD is hydroelectric and pumped storage, NU is nuclear, ST is steam turbine.

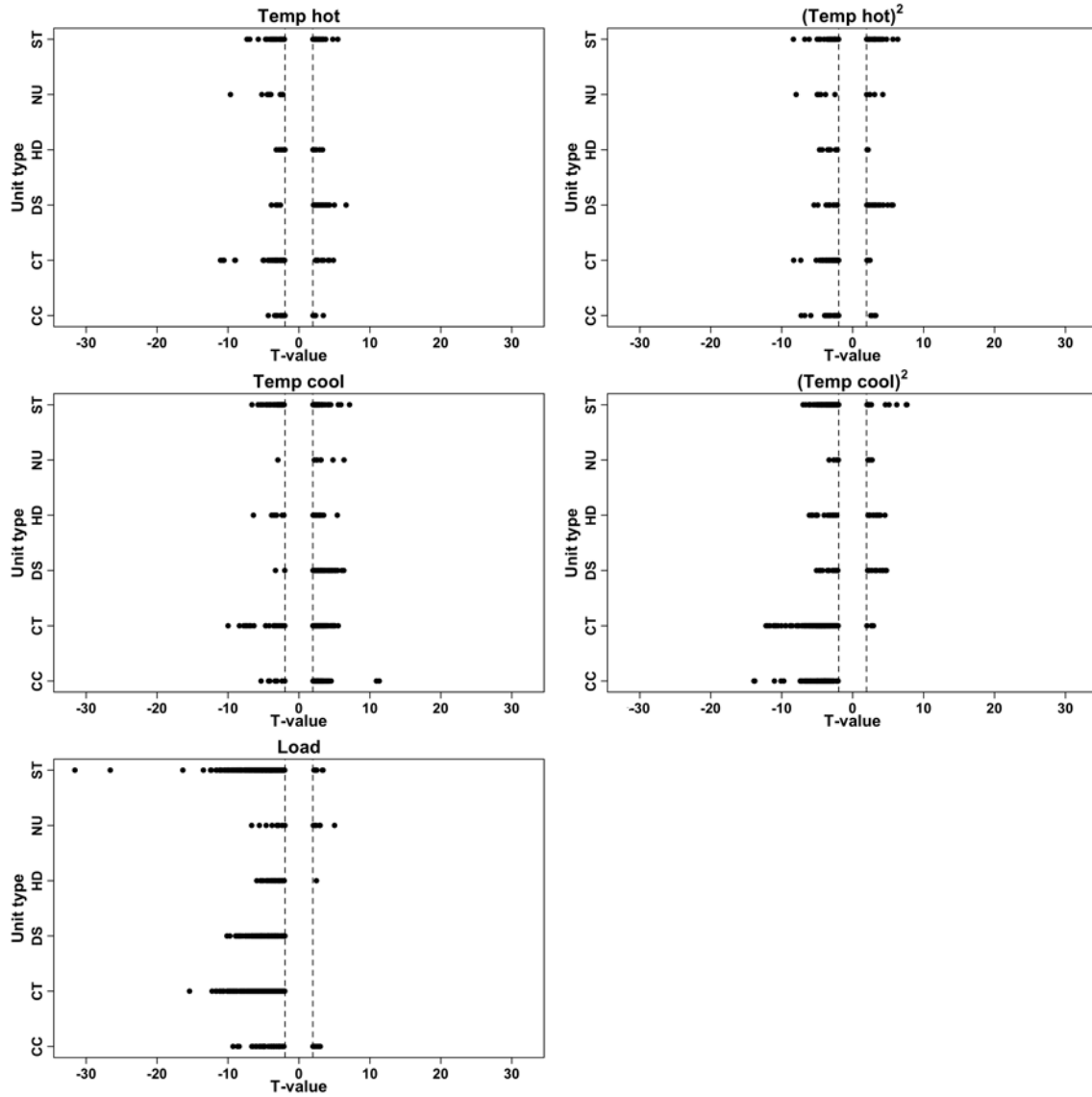


Figure A.4: Summarizing t-values for the available model by covariate and generator type (1995-2018 model fits). Only generators for which the covariate is statistically significant at the 0.05 level are included. Thresholds for significance (± 1.96) indicated by dashed vertical lines. Constants are excluded. CC is combined cycle, CT is simple cycle, DS is diesel, HD is hydroelectric and pumped storage, NU is nuclear, ST is steam turbine.

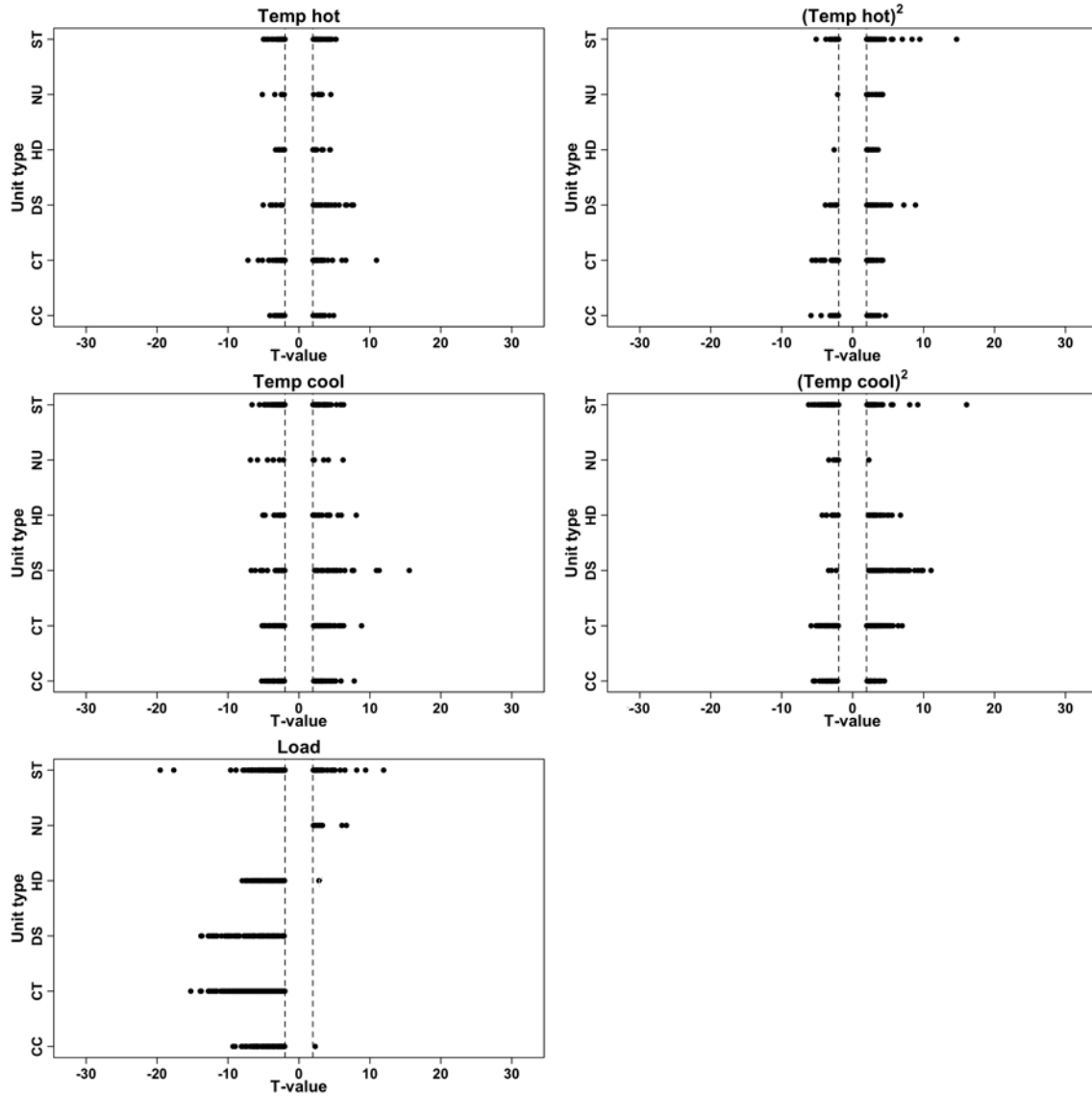


Figure A.5: Summarizing t-values for the derated model by covariate and generator type (1995-2018 model fits). Only generators for which the covariate is statistically significant at the 0.05 level are included. Thresholds for significance (± 1.96) indicated by dashed vertical lines. Constants are excluded. CC is combined cycle, CT is simple cycle, DS is diesel, HD is hydroelectric and pumped storage, NU is nuclear, ST is steam turbine.

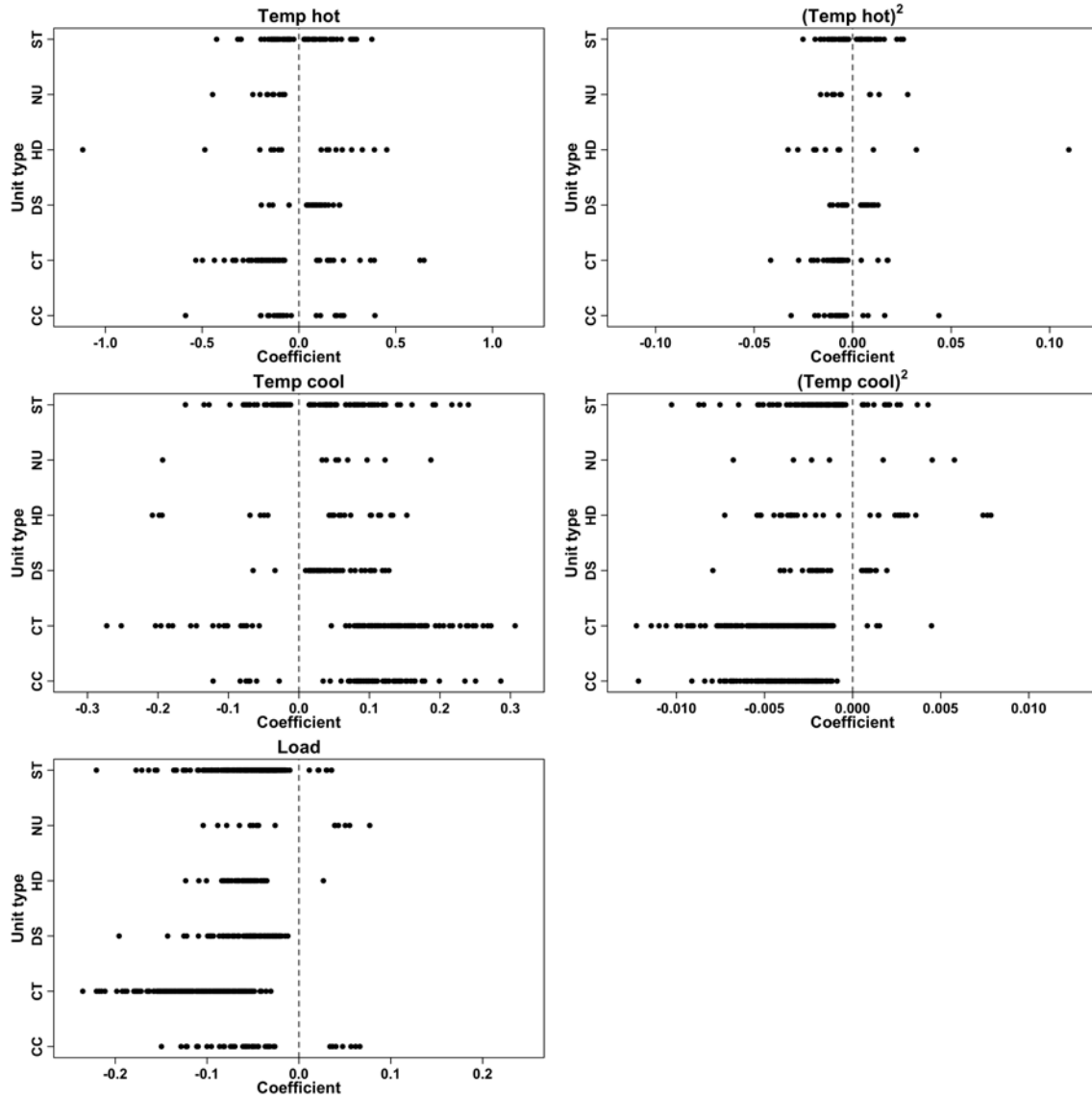


Figure A.6: Summarizing coefficients for the available model by covariate and generator type (1995-2018 model fits). Only generators for which the covariate is statistically significant at the 0.05 level are included. Dashed vertical lines indicate 0. Constants are excluded. Temperature units are degrees Celsius. Load units are GW. Abscissa scales set independently. CC is combined cycle, CT is simple cycle, DS is diesel, HD is hydroelectric and pumped storage, NU is nuclear, ST is steam turbine.

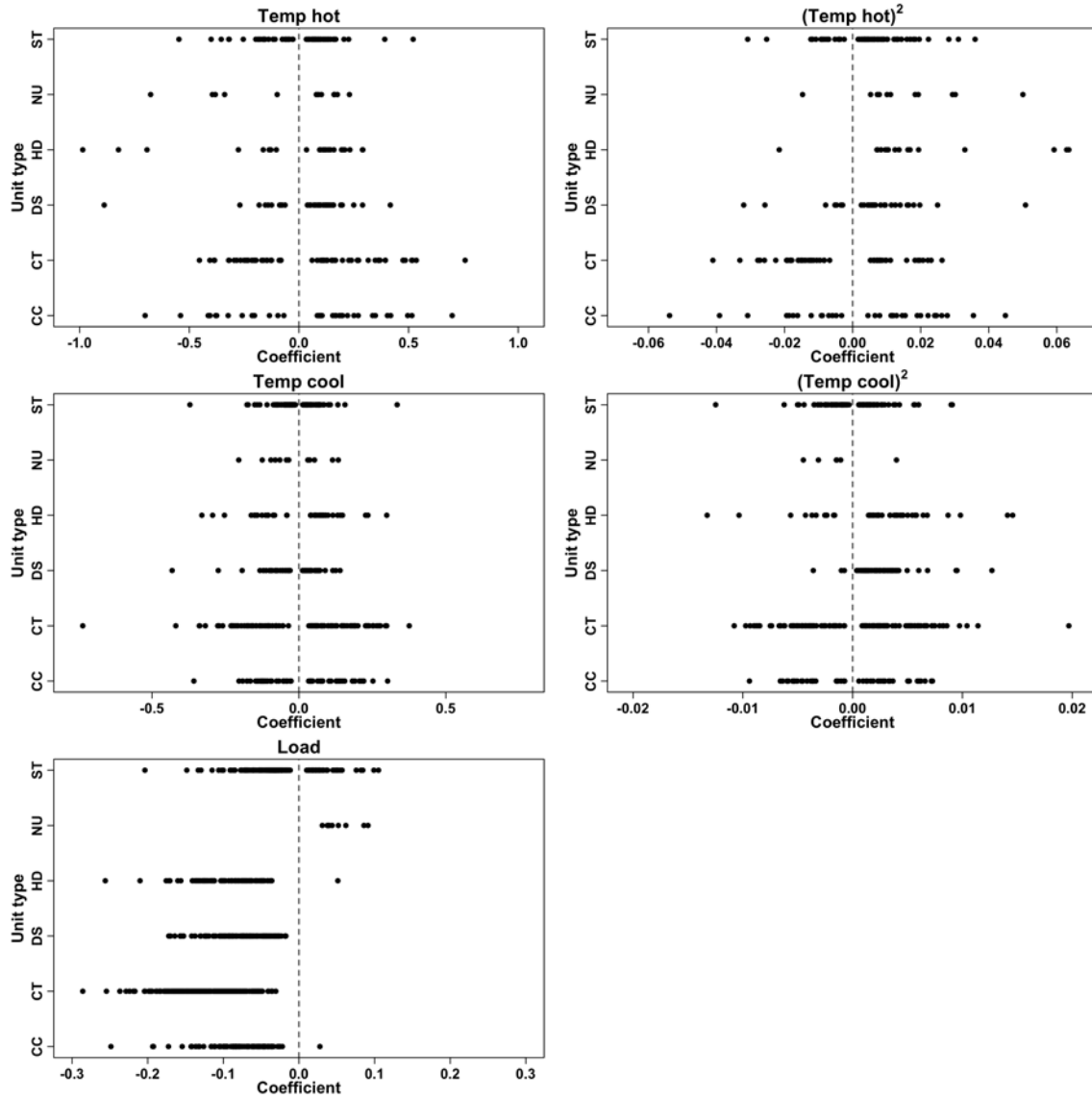


Figure A.7: Summarizing coefficients for the derated model by covariate and generator type (1995-2018 model fits). Only generators for which the covariate is statistically significant at the 0.05 level are included. Dashed vertical lines indicate 0. Constants are excluded. Temperature units are degrees Celsius. Load units are GW. Abscissa scales set independently. CC is combined cycle, CT is simple cycle, DS is diesel, HD is hydroelectric and pumped storage, NU is nuclear, ST is steam turbine.

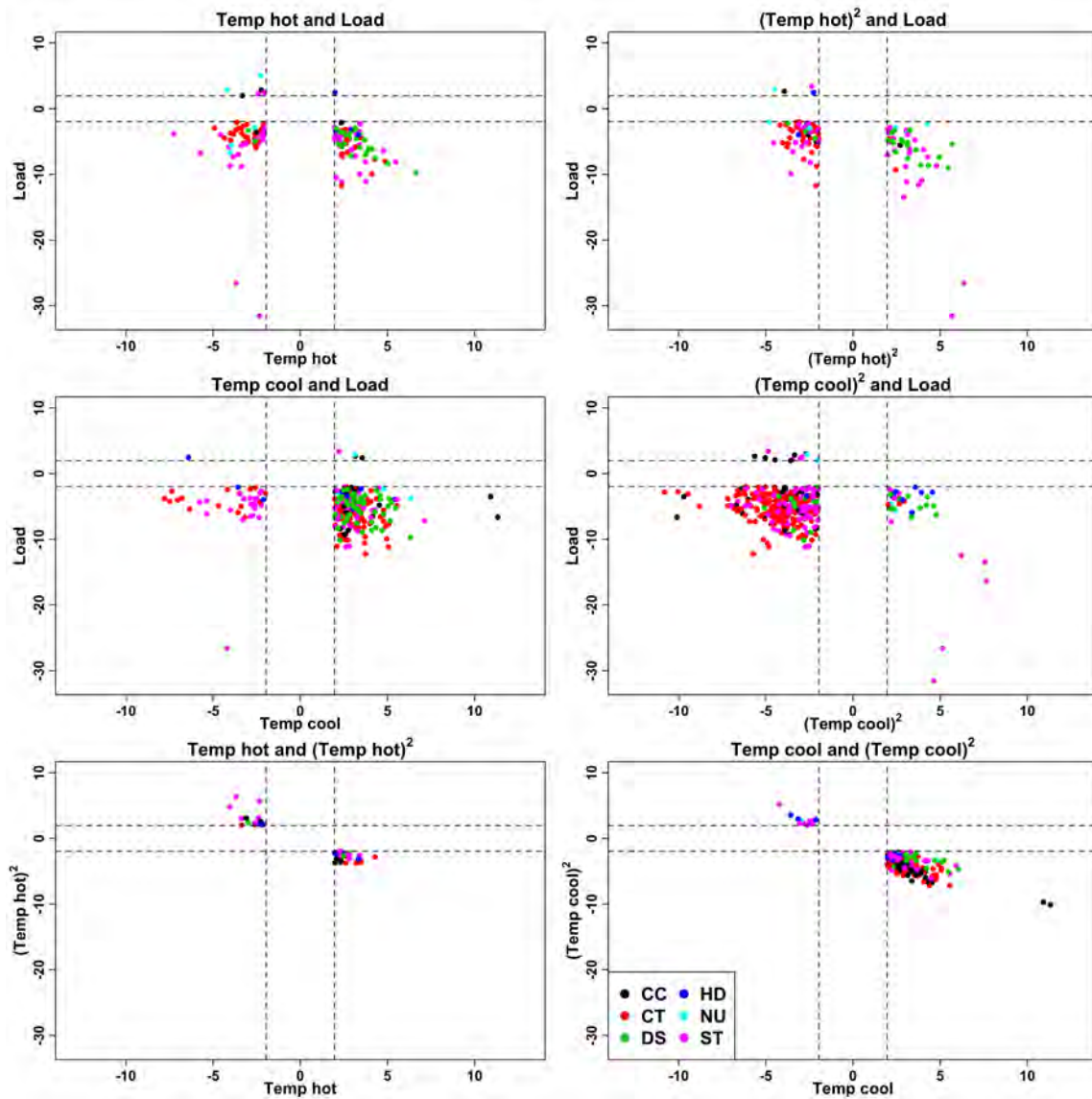


Figure A.8: Summarizing t -value relationships for non-orthogonal covariate pairs for the available model (1995-2018 model fits). Thresholds for significance at 0.05 level (± 1.96) indicated by dashed red lines. To be included in a plot in this figure, both relevant covariates must be present in the final available model. Black is combined cycle gas (CC), red is simple cycle gas (CT), green is diesel (DS), blue is hydroelectric (HD), cyan is nuclear (NU), magenta is steam turbine (ST).

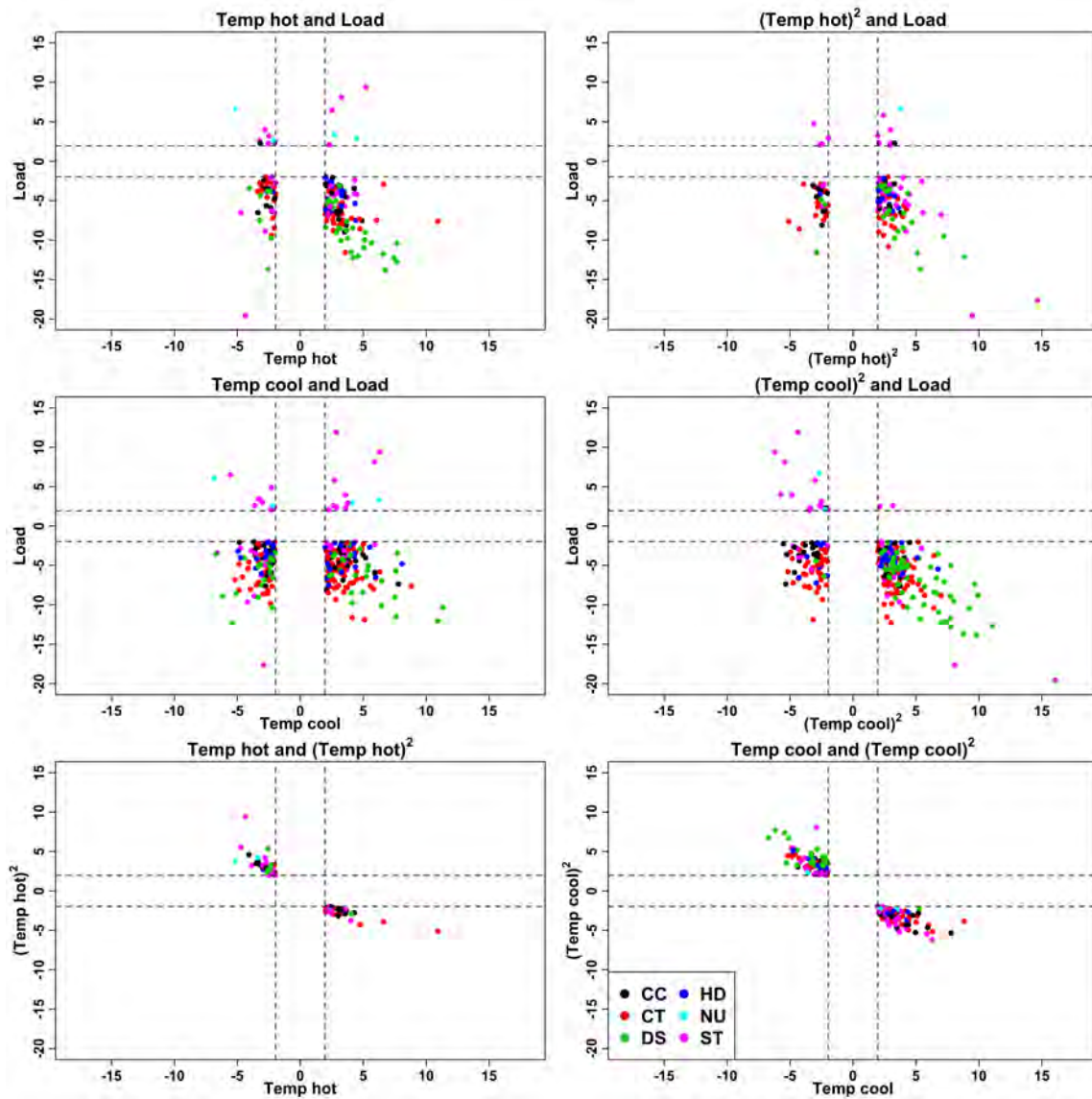


Figure A.9: Summarizing t-value relationships for non-orthogonal covariate pairs for the derated model (1995-2018 model fits). Thresholds for significance at 0.05 level (+/- 1.96) indicated by dashed red lines. To be included in a plot in this figure, both relevant covariates must be present in the final derated model. Black is combined cycle gas (CC), red is simple cycle gas (CT), green is diesel (DS), blue is hydroelectric (HD), cyan is nuclear (NU), magenta is steam turbine (ST).

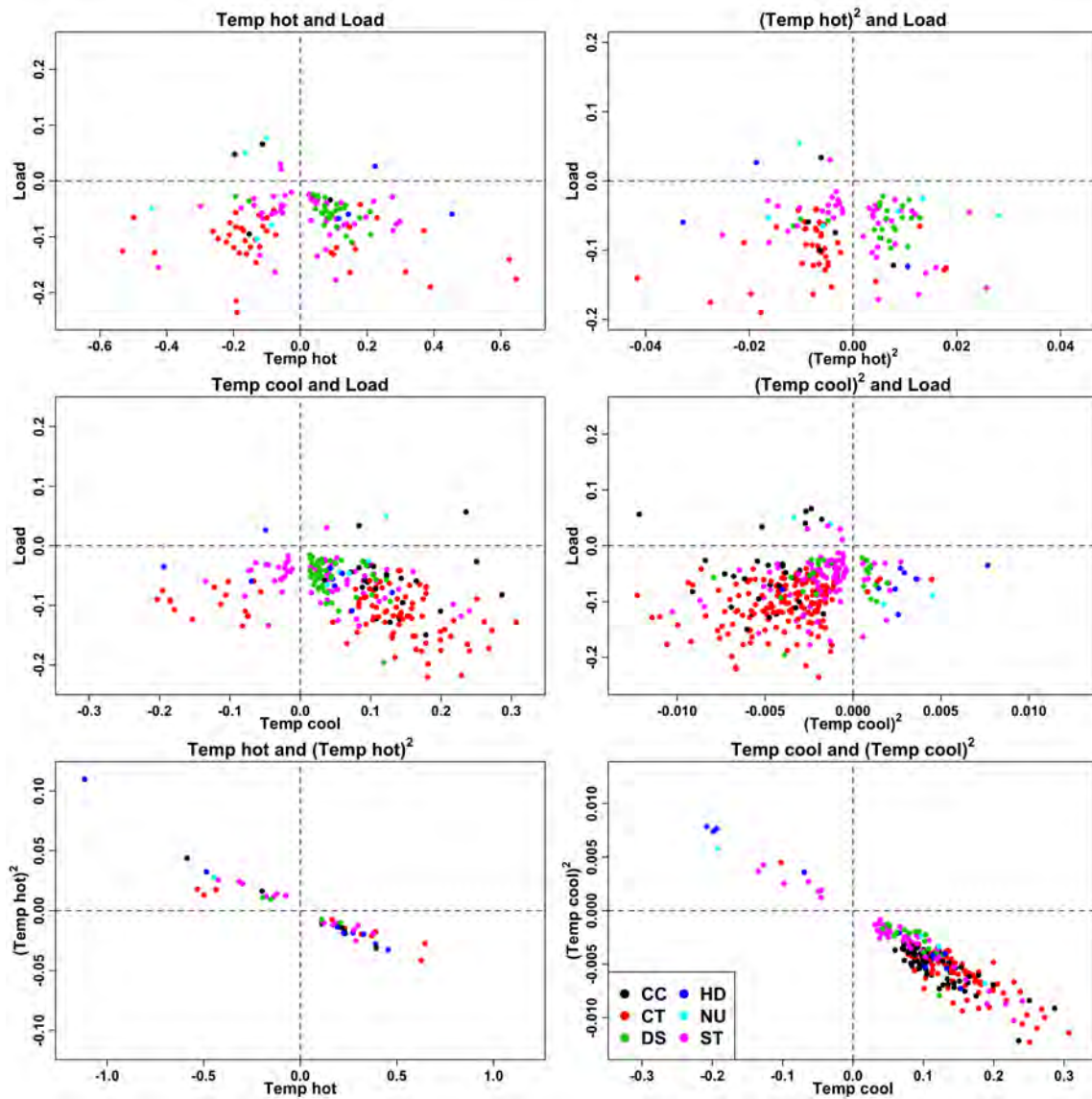


Figure A.10: Summarizing coefficient relationships for non-orthogonal covariate pairs for the available model (1995-2018 model fits). To be included in a plot in this figure, both relevant covariates must be present in the final available model. Black is combined cycle gas (CC), red is simple cycle gas (CT), green is diesel (DS), blue is hydroelectric (HD), cyan is nuclear (NU), magenta is steam turbine (ST). Dashed lines indicate 0. Temperature units are degrees C. Load units are GW. Axis scales set independently in each plot.

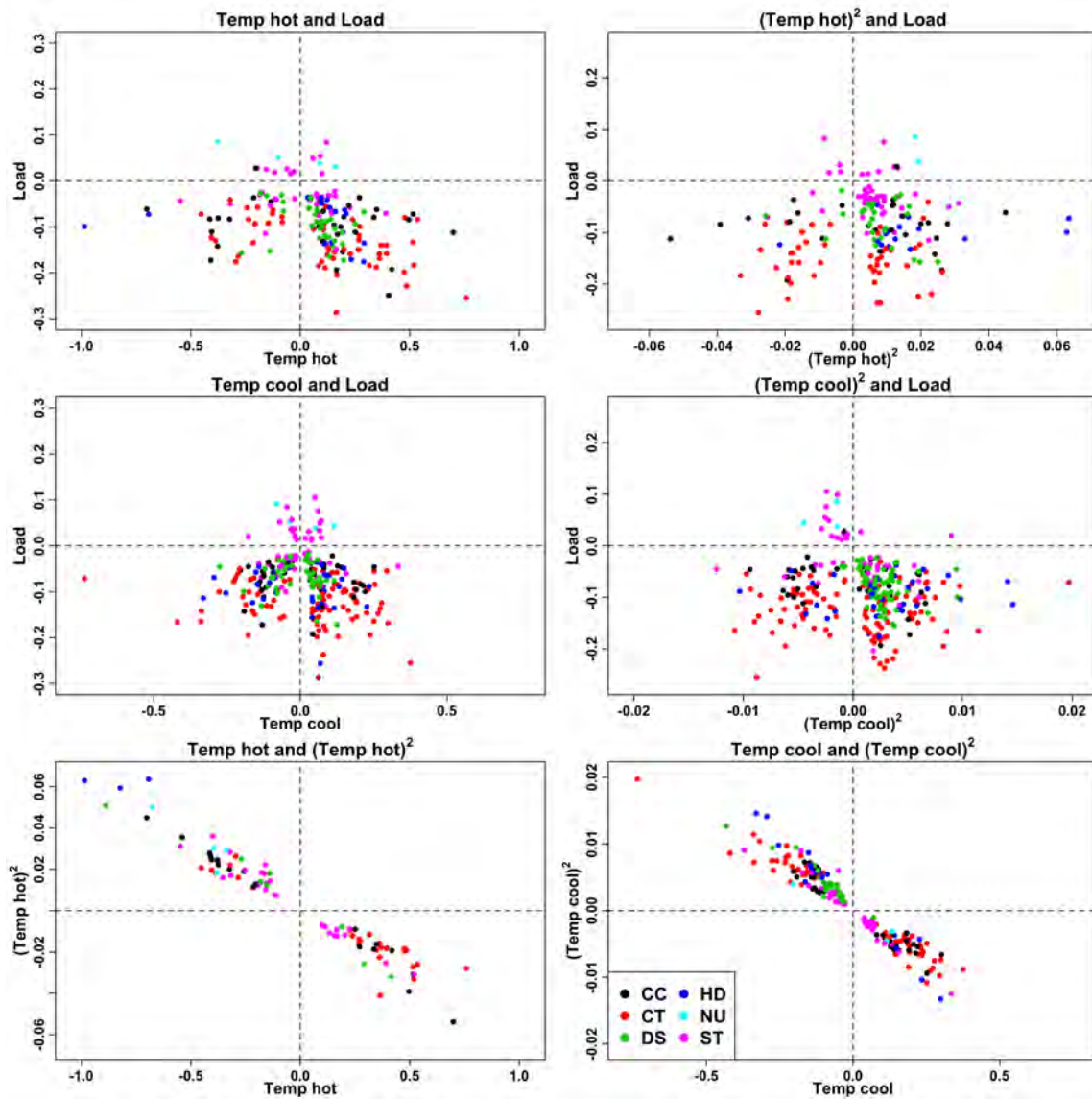


Figure A.11: Summarizing coefficient relationships for non-orthogonal covariate pairs for the derated model (1995-2018 model fits). To be included in a plot in this figure, both relevant covariates must be present in the final derated model. Black is combined cycle gas (CC), red is simple cycle gas (CT), green is diesel (DS), blue is hydroelectric (HD), cyan is nuclear (NU), magenta is steam turbine (ST). Dashed lines indicate 0. Temperature units are degrees C. Load units are GW. Axis scales set independently in each plot.

Model	0	1	2	3	4	5	6	7
Available	0	1	125	338	338	236	64	9
Derated	0	2	130	366	294	235	72	12

Table A.3: Number of statistically significant parameters (including constants) for the 1,111 generators with at least 10 instances of the less-common transition per parameter in both available and derated models (1995-2018 model fits).

Model	0	1	2	3	4
Available	346	341	323	84	17
Derated	365	351	288	88	19

Table A.4: Number of statistically significant temperature parameters (excluding constants) for the 1,111 generators with at least 10 instances of the less-common transition per parameter in both available and derated models (1995-2018 model fits).

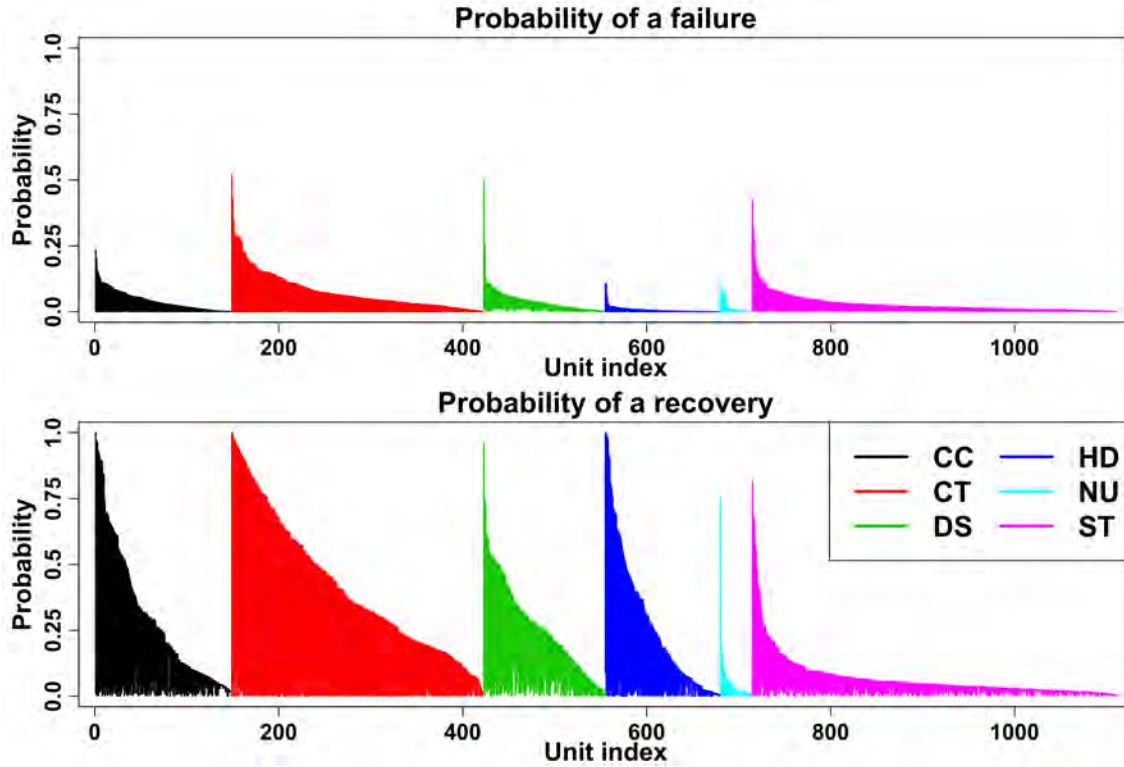


Figure A.12: Summarizing the empirical range of hourly transition probabilities (1995-2018 model fits). Plots include 1,111 generators with at least 10 failure and recovery events per statistically significant model parameter. Each generator is represented as a vertical line at an integer index (1 to 1,111). In each plot, generators are sorted by generator type and maximum experienced transition probability. Black is combined cycle gas (CC), red is simple cycle gas (CT), green is diesel (DS), blue is hydroelectric (HD), cyan is nuclear (NU), magenta is steam turbine (ST).

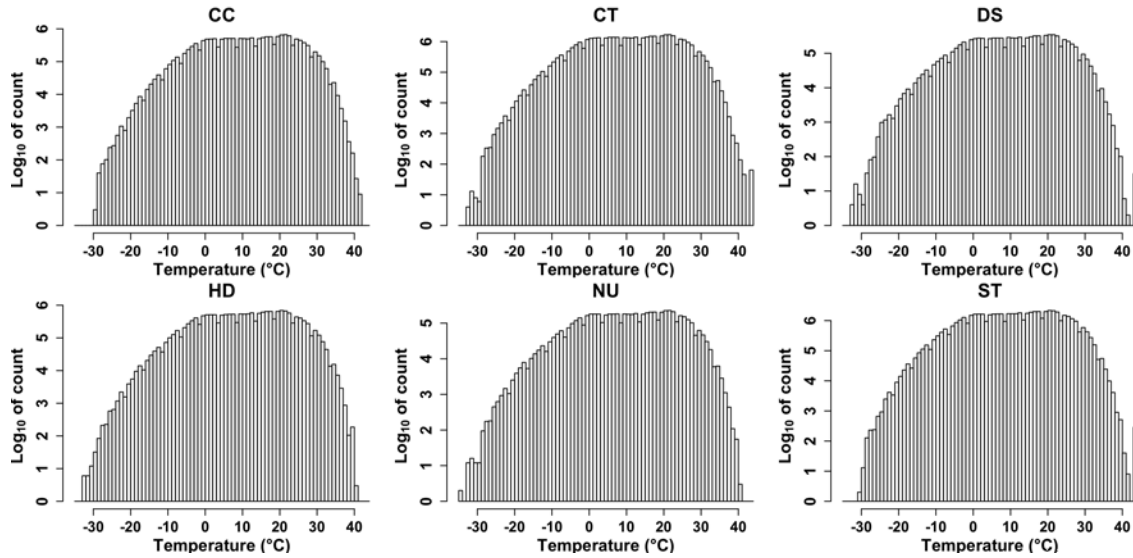


Figure A.13: Prevalence of temperatures experienced by 1,111 modeled generators by generator type (1995-2018 model fits). For use in conjunction with Figure 6. Note the log scale on the ordinate. CC is combined cycle, CT is simple cycle, DS is diesel, HD is hydroelectric and pumped storage, NU is nuclear, ST is steam turbine.

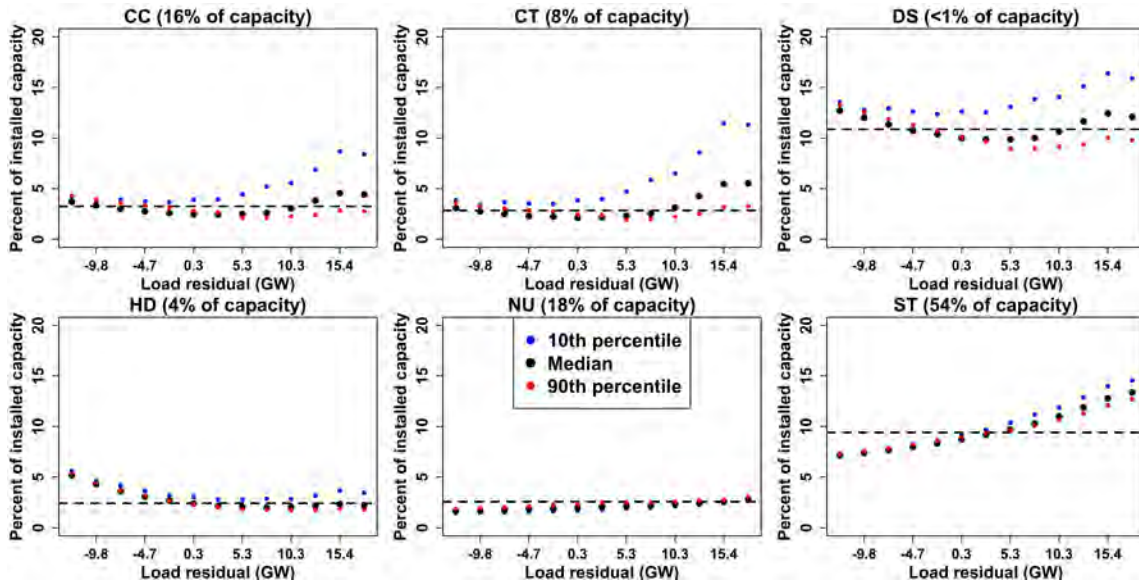


Figure A.14: Expected levels of unavailable capacity as a function of load under logistic regression (dots) and current practice (dashed horizontal line) when restricting to temperatures below 18.3 degrees Celsius (1995-2018 model fits). Black dots computed at median temperature from load neighborhood; blue and red dots correspond to 10th and 90th percentile temperatures from load neighborhood, respectively. Load neighborhood defined analogously to temperature neighborhood of Figure 6. Current practice dashed line matches that of Figure 6. Plot domain defined using only observations below 18.3 degrees. CC is combined cycle, CT is simple cycle, DS is diesel, HD is hydroelectric and pumped storage, NU is nuclear, ST is steam turbine.

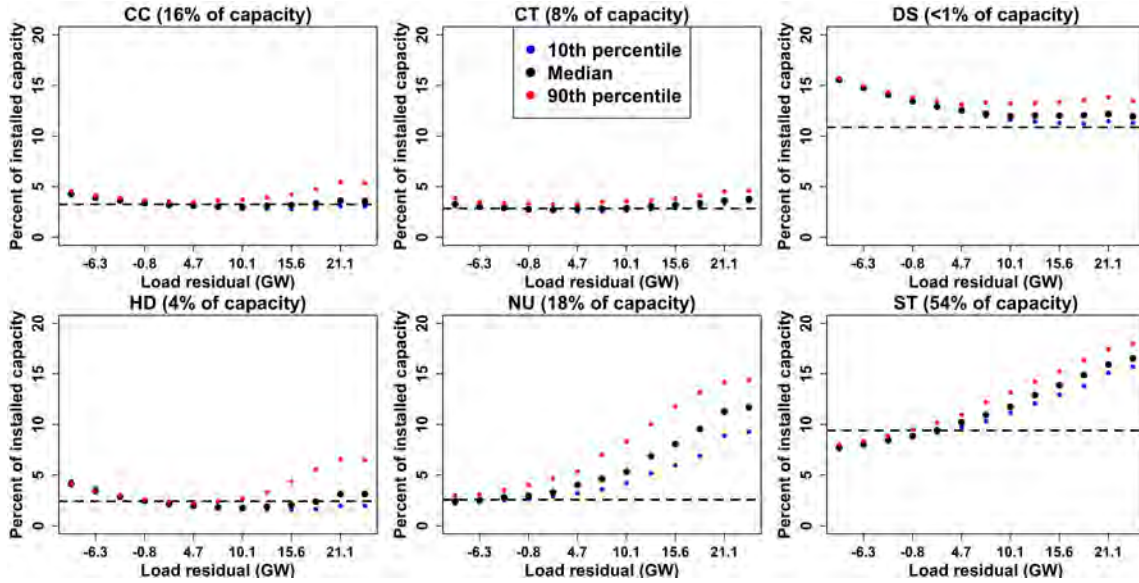


Figure A.15: Expected levels of unavailable capacity as a function of load under logistic regression (dots) and current practice (dashed horizontal line) when restricting to temperatures above 18.3 degrees Celsius (1995-2018 model fits). Black dots computed at median temperature from load neighborhood; blue and red dots correspond to 10th and 90th percentile temperatures from load neighborhood, respectively. Load neighborhood defined analogously to temperature neighborhood of Figure 6. Current practice dashed line matches that of Figure 6. Plot domain defined using only observations above 18.3 degrees. CC is combined cycle, CT is simple cycle, DS is diesel, HD is hydroelectric and pumped storage, NU is nuclear, ST is steam turbine.

Appendix B: Figures and tables for 2004-2018 model fits

As discussed in Section 3.2.4 of the main text, there was incomplete reporting of reserve shutdown (RS) events to PJM GADS prior to 2004. RS events are used to indicate when a generator is offline for economic reasons rather than due to a failure event. If one assumes that the incidence of a failure while a generator is not operating and not being repaired is much lower than when operating or when being repaired, reserve shutdown hours should be excluded from both available and derated model fits. However, given that most generators fail infrequently and that we require a minimum of 10 *AD* and *DA* transitions per statistically significant covariate to keep a generator in our analysis, eliminating the first nine years of data results in significantly fewer generators retained. As a result, we fit our models twice: once using the full data reporting period for all generators (results presented in the main text and in Appendix A) and once discarding all data prior to 2004 (results presented here).

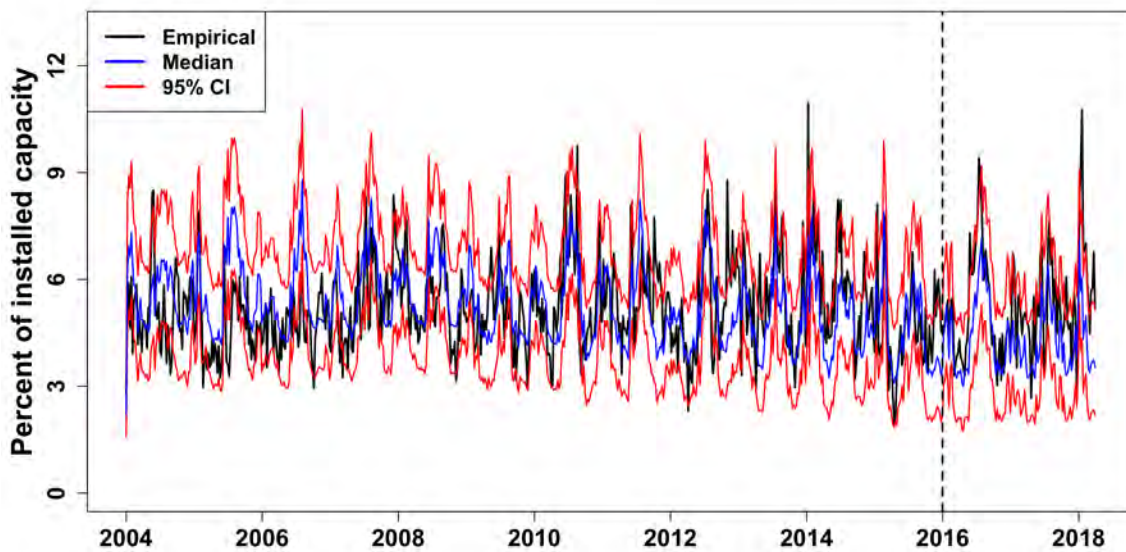


Figure B.1: Simulated time series from logistic regression model (2004-2015 model fits). Results presented for 703 generators with sufficient state transitions to support their available and derated models when fitting on 2004-2015; 2016-2018 used as test of model performance. The split between training and testing periods is denoted with a dashed vertical line. Weekly averages rather than hourly series. 5000 simulations conducted. Refer to Table B.1 for installed capacity by calendar year. Black trace is the empirical time series; blue trace is the concatenation of pointwise median simulation values; red traces are the concatenation of pointwise 2.5% and 97.5% simulation values.

Year	CC	CT	DS	HD	NU	ST	All
2004	14.8	1.6	0.1	2.9	31.8	79.3	130.5
2005	19.5	1.6	0.1	3.0	33.2	92.1	149.4
2006	20.4	1.6	0.1	3.0	33.2	92.3	150.5
2007	21.9	1.6	0.1	3.0	33.2	99.4	159.2
2008	23.1	1.6	0.1	3.0	33.2	98.8	159.9
2009	23.5	1.6	0.2	3.0	33.2	98.4	159.9
2010	23.3	1.8	0.2	3.0	33.2	98.7	160.1
2011	23.2	1.8	0.2	3.1	33.2	98.6	159.9
2012	25.1	1.8	0.2	3.1	33.2	92.6	155.9
2013	25.4	1.8	0.3	3.1	33.2	92.6	156.2
2014	25.4	1.8	0.3	3.1	33.2	91.0	154.6
2015	25.3	1.3	0.3	3.1	33.2	83.2	146.4
2016	25.3	1.3	0.3	3.1	33.2	82.2	145.4
2017	25.1	1.3	0.3	3.1	33.2	80.2	143.0
2018	25.1	1.3	0.3	3.1	33.2	80.2	143.0

Table B.1: Installed capacity (GW) of 703 retained generators by year and generator type (2004-2015 model fits). For use in conjunction with Figure B.1. CC is combined cycle, CT is simple cycle, DS is diesel, HD is hydroelectric and pumped storage, NU is nuclear, ST is steam turbine.

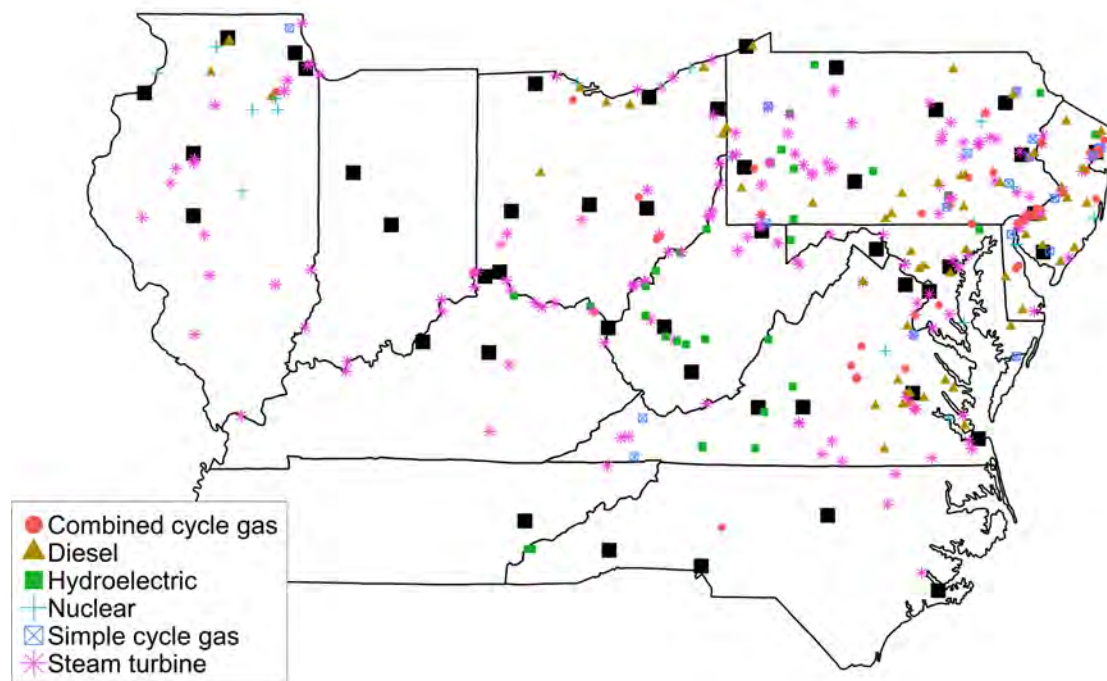


Figure B.2: Locations of 748 generators and linked weather stations, overlaid on corresponding U.S. states (2004-2018 model fits). Only generators with 10 transitions per statistically significant model parameter when fitting models using 2004-2018 data are retained. Note that all generators in multi-generator power plants have identical locations. Large black squares indicate weather stations. A small number of retained generators are not shown for presentation considerations: Alabama (2), Louisiana (3), Michigan (12), Mississippi (3), South Carolina (1), Texas (7).

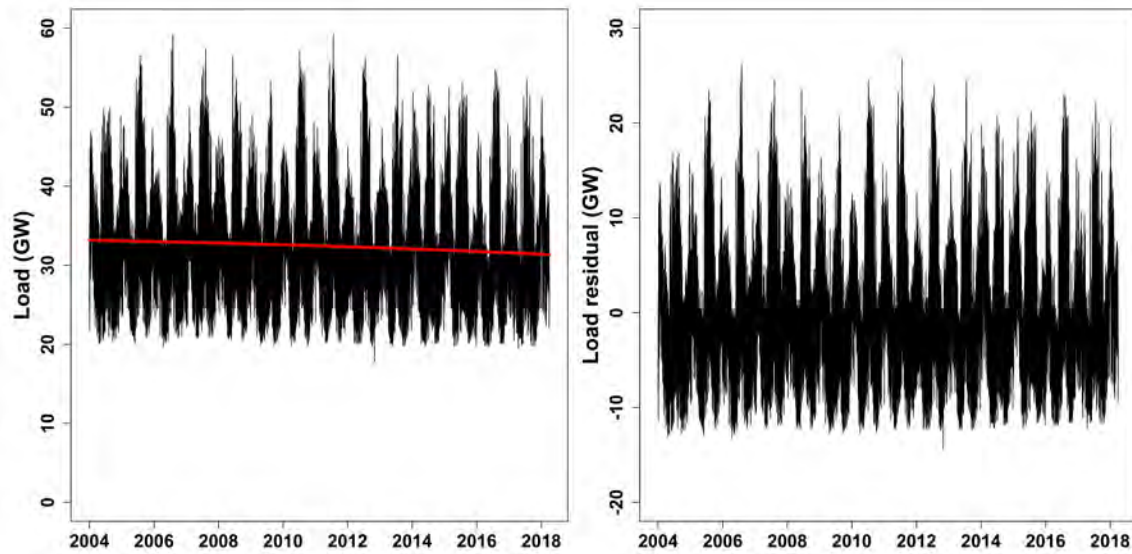


Figure B.3: Metered load time series (2004-2018 model fits). Left: hourly time series of metered system load for PJM transmission zones that have been part of PJM since database inception, with time trend (red curve) as described in Section 3.3.3. Right: residuals from fitting time trend to the original series.

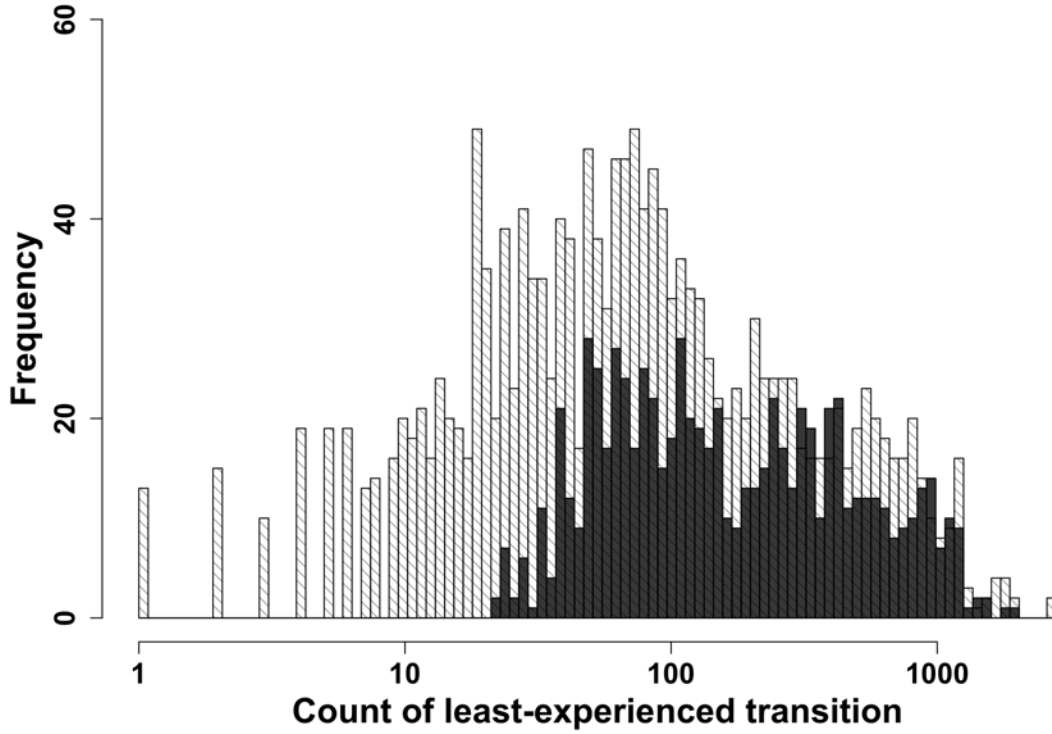


Figure B.4: Histogram of the count of least frequently experienced transition by generator (2004-2018 model fits). The 1,748 generators with at least one full calendar year of data reporting and at least one unscheduled transition during 1995-2018 are plotted in light gray (consistent with Figure A.3). Of these, the 748 generators with at least 10 failure and recovery transitions per statistically significant parameter during 2004-2018 are then overplotted in dark gray. In contrast to Figure A.3, not all generators with at least 70 failure and recovery transitions are retained due to the more restrictive time period. Note the log scale on the abscissa.

Generator type	Total count	Retained count (%)	Total capacity	Retained capacity (%)
CC	224	126 (56)	53.4	31.2 (58)
CT	663	44 (7)	44.9	1.9 (4)
DS	236	120 (51)	0.8	0.4 (46)
HD	244	68 (28)	11.0	4.2 (38)
NU	35	32 (91)	37.2	34.2 (92)
ST	443	358 (81)	119.5	106.4 (89)
All	1,845	748 (41)	266.8	178.3 (67)

Table B.2: Summary of total and retained generator counts and capacity, by generator type (2004-2018 model fits). Only generators with at least 10 failure and recovery transitions per statistically significant model parameter are retained. Capacity reported in GW. CC is combined cycle, CT is simple cycle, DS is diesel, HD is hydroelectric and pumped storage, NU is nuclear, ST is steam turbine.

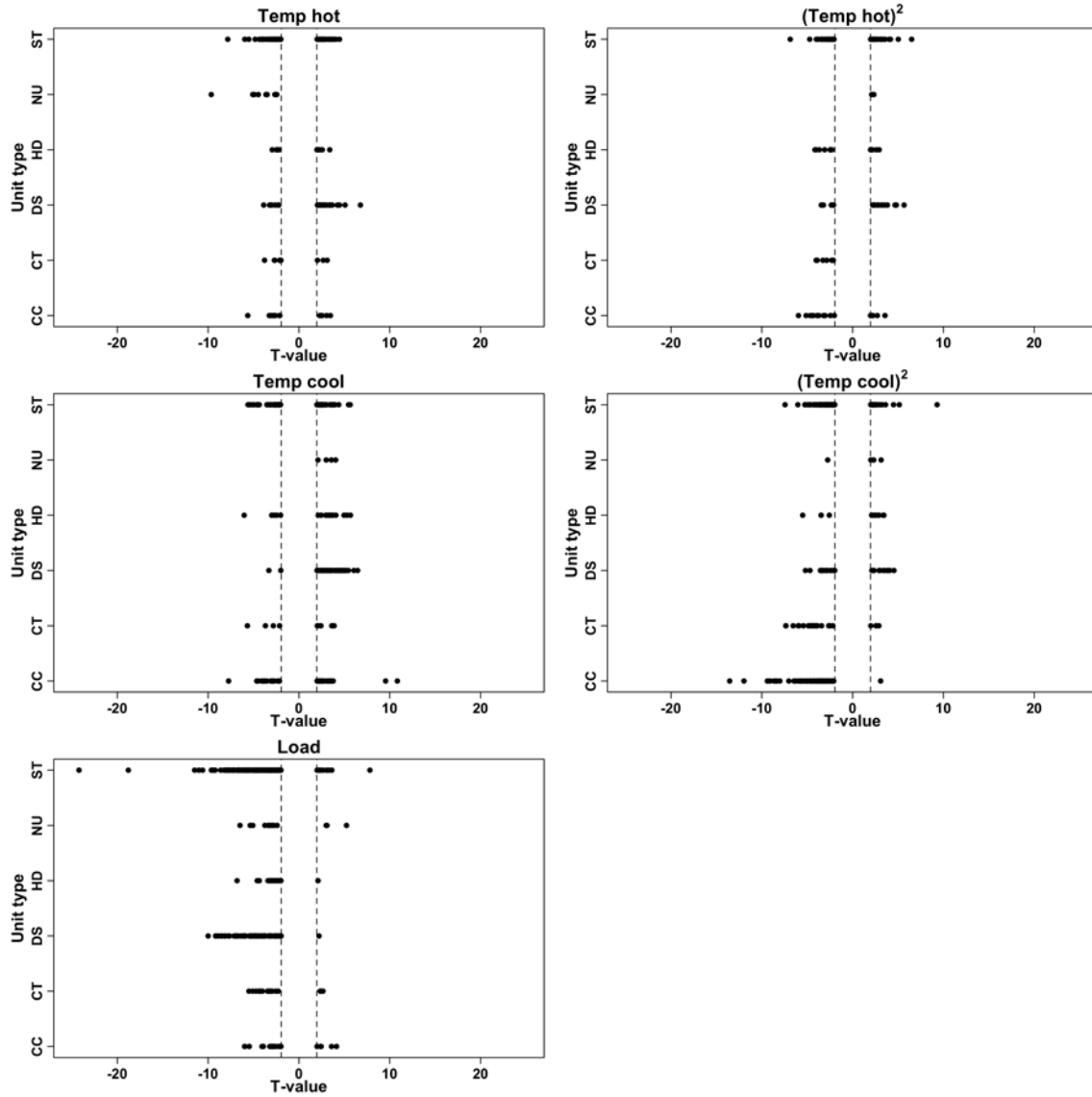


Figure B.5: Summarizing t-values for the available model by covariate and generator type (2004-2018 model fits). Only generators for which the covariate is statistically significant at the 0.05 level are included. Thresholds for significance (± 1.96) indicated by dashed vertical lines. Constants are excluded. CC is combined cycle, CT is simple cycle, DS is diesel, HD is hydroelectric and pumped storage, NU is nuclear, ST is steam turbine.

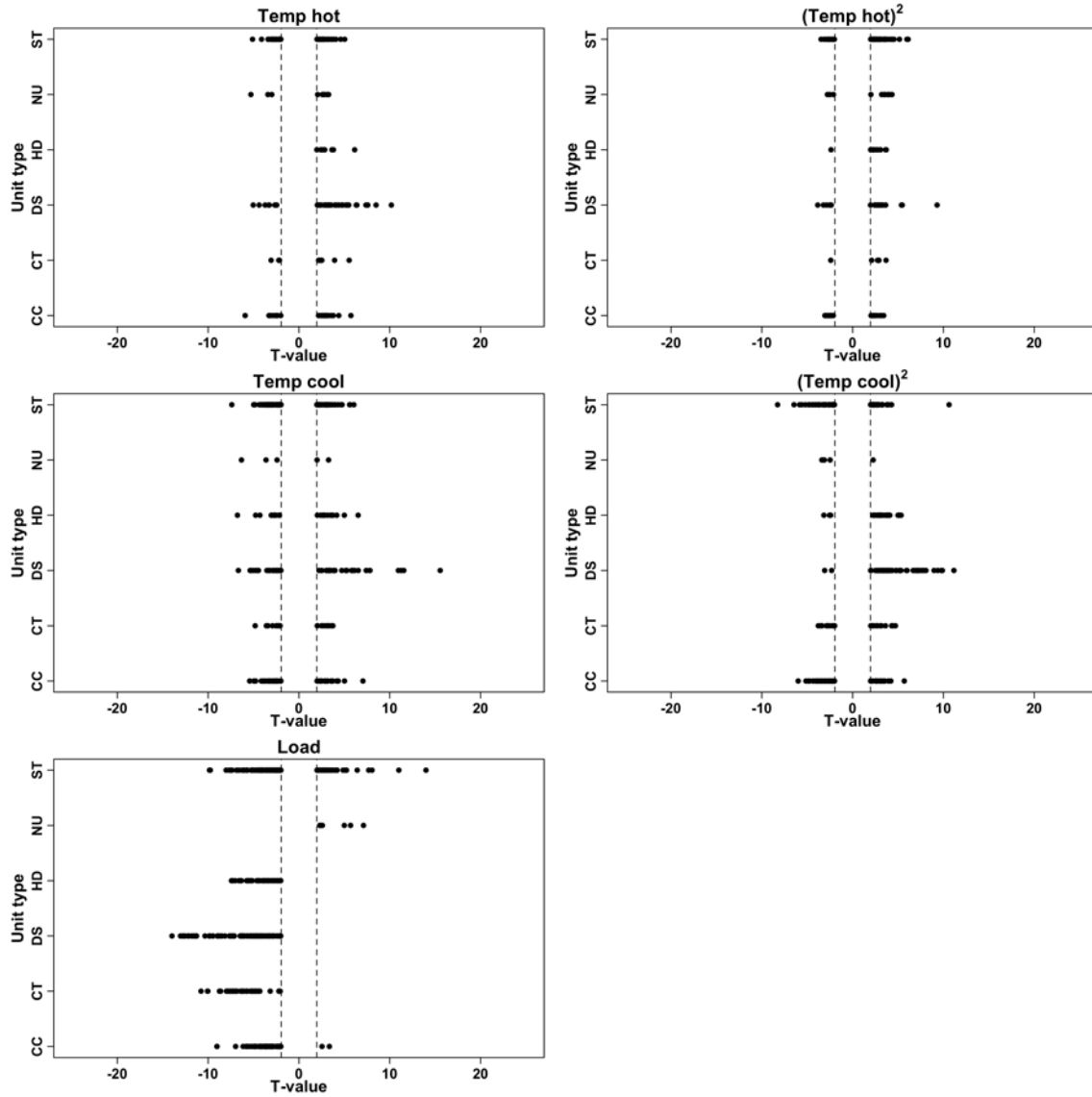


Figure B.6: Summarizing t-values for the derated model by covariate and generator type (2004-2018 model fits). Only generators for which the covariate is statistically significant at the 0.05 level are included. Thresholds for significance (± 1.96) indicated by dashed vertical lines. Constants are excluded. CC is combined cycle, CT is simple cycle, DS is diesel, HD is hydroelectric and pumped storage, NU is nuclear, ST is steam turbine.

Generator type	Count	Mean hot	Mean cool	Temp hot	Temp hot ²	Temp cool	Temp cool ²	Load
CC	126	126	126	17	21	43	80	21
CT	44	44	44	9	6	11	26	16
DS	120	120	120	36	29	57	27	93
HD	68	68	68	11	13	17	12	31
NU	32	32	32	9	2	4	4	12
ST	358	358	358	68	53	84	91	204
All	748	748	748	150	124	216	240	377

Table B.3: Number of times each model term is statistically significant at the 95% level for the available model (2004-2018 model fits). Results reported for the 748 generating generators with at least 10 instances of the less-common transition per parameter in both available and derated models.

Generator type	Count	Mean hot	Mean cool	Temp hot	Temp hot ²	Temp cool	Temp cool ²	Load
CC	126	124	126	26	27	52	47	69
CT	44	44	44	9	6	18	20	39
DS	120	120	119	41	24	55	62	100
HD	68	67	67	8	15	23	26	56
NU	32	32	32	9	10	5	5	6
ST	358	358	358	58	66	111	87	128
All	748	745	746	151	148	264	247	398

Table B.4: Number of times each model term is statistically significant at the 95% level for the derated model (2004-2018 model fits). Results reported for the 748 generating generators with at least 10 instances of the less-common transition per parameter in both available and derated models.

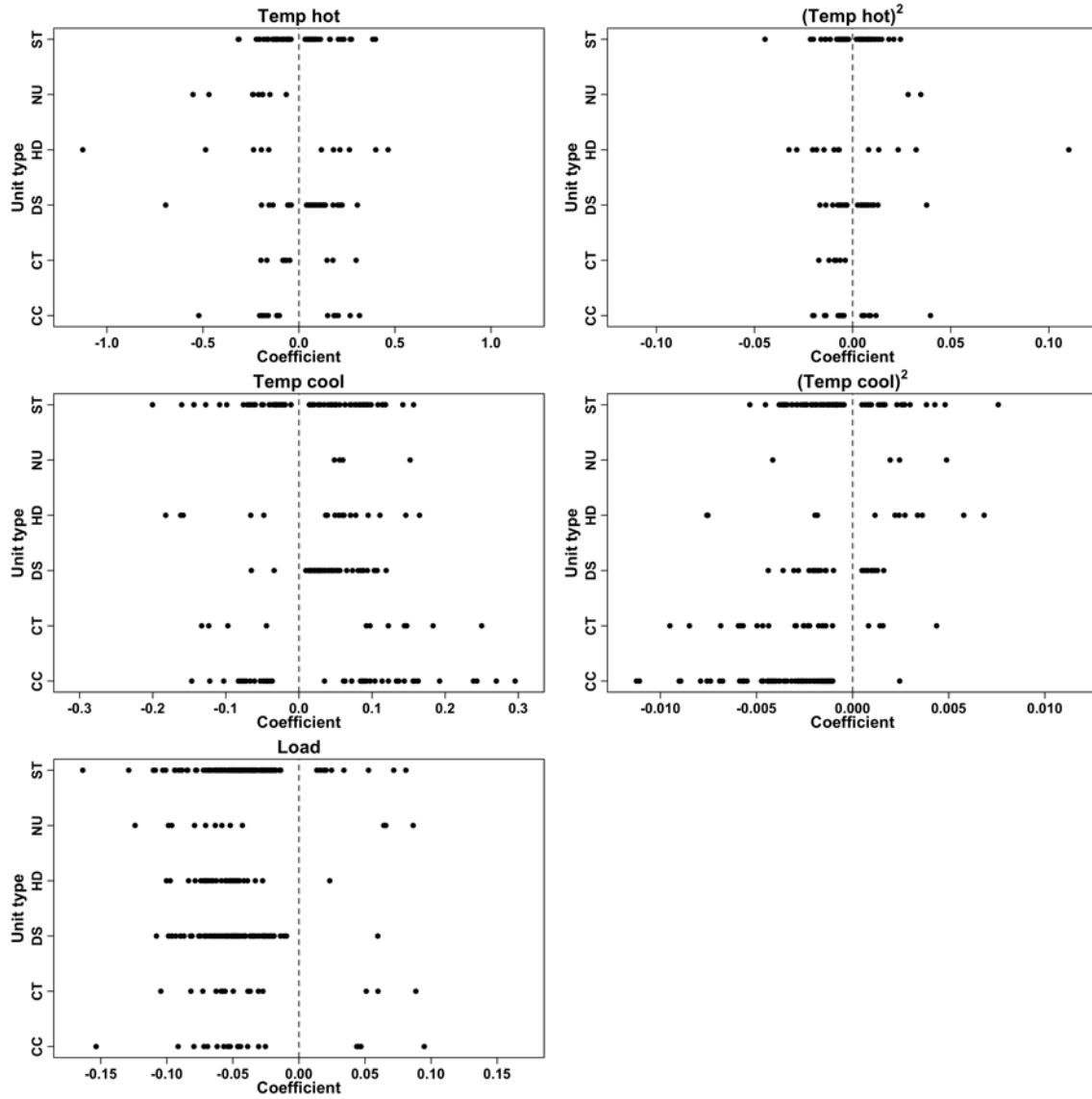


Figure B.7: Summarizing coefficients for the available model by covariate and generator type (2004-2018 model fits). Only generators for which the covariate is statistically significant at the 0.05 level are included. Dashed vertical lines indicate 0. Constants are excluded. Temperature units are degrees C. Load units are GW. Abscissa scales set independently. CC is combined cycle, CT is simple cycle, DS is diesel, HD is hydroelectric and pumped storage, NU is nuclear, ST is steam turbine.

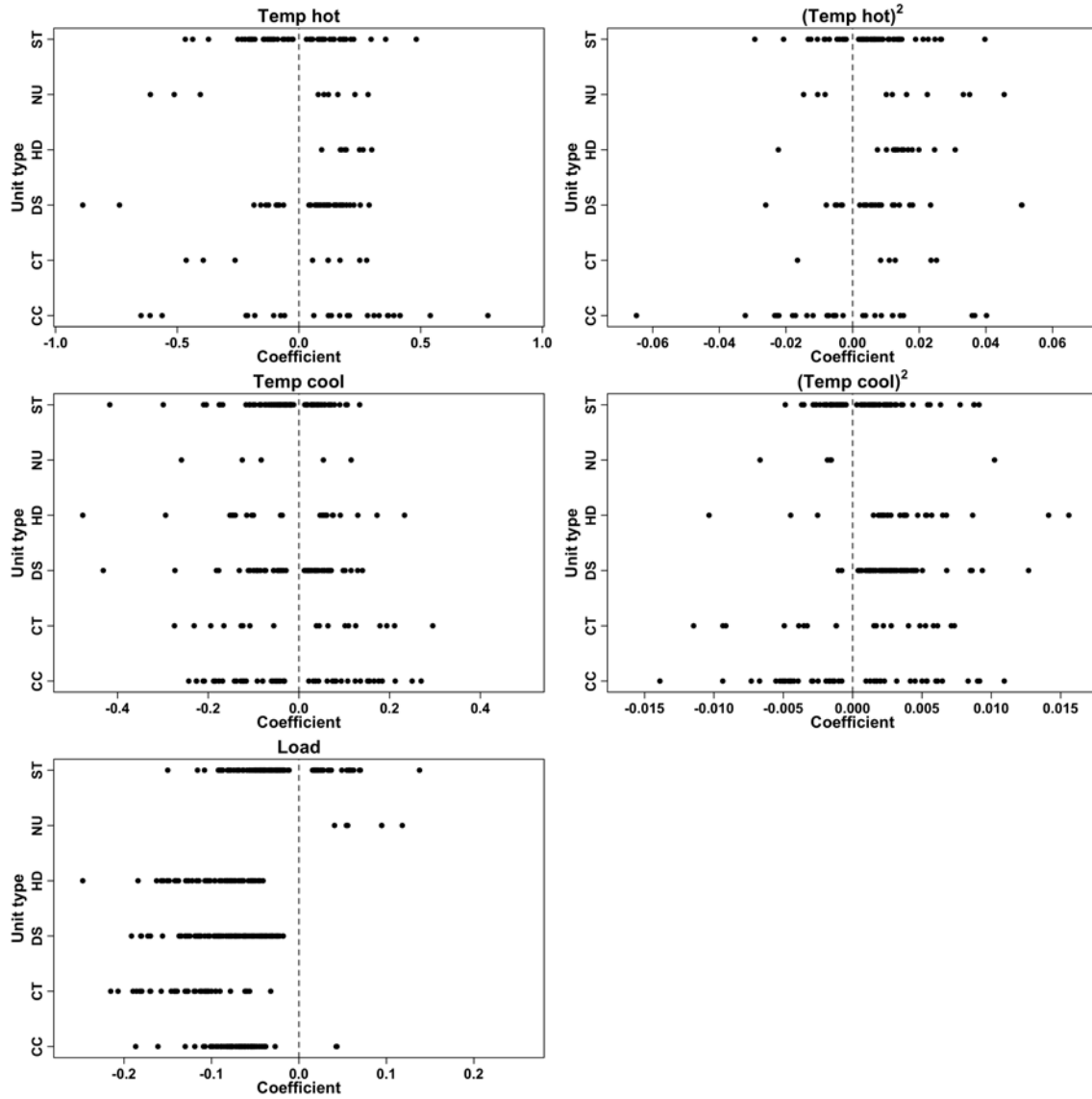


Figure B.8: Summarizing coefficients for the derated model by covariate and generator type (2004-2018 model fits). Only generators for which the covariate is statistically significant at the 0.05 level are included. Dashed vertical lines indicate 0. Constants are excluded. Temperature units are degrees C. Load units are GW. Abscissa scales set independently. CC is combined cycle, CT is simple cycle, DS is diesel, HD is hydroelectric and pumped storage, NU is nuclear, ST is steam turbine.

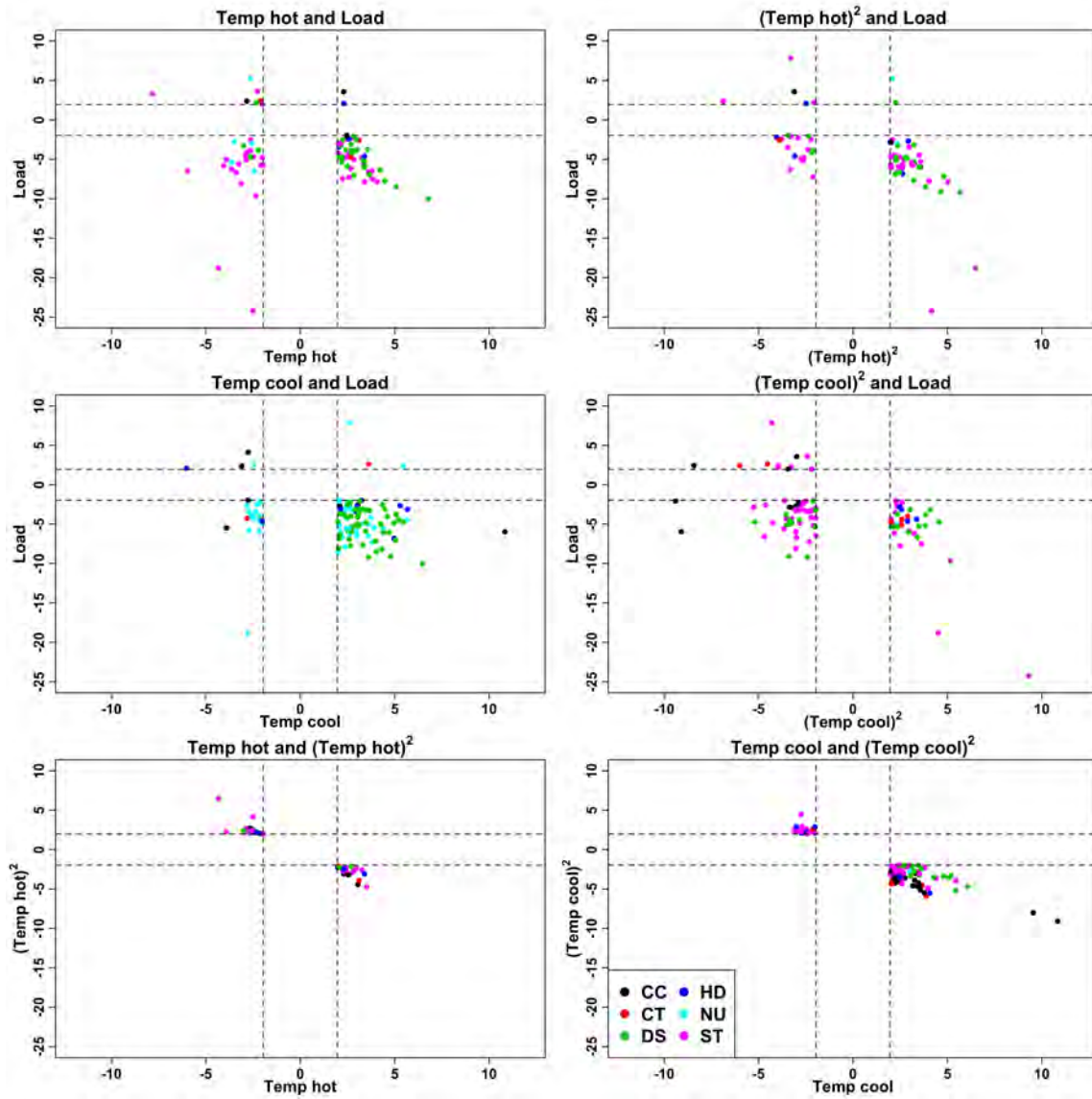


Figure B.9: Summarizing t-value relationships for non-orthogonal covariate pairs for the available model (2004-2018 model fits). Thresholds for significance at 0.05 level (± 1.96) indicated by dashed lines. To be included in a plot in this figure, both relevant covariates must be present in the final available model. Black is combined cycle gas (CC), red is simple cycle gas (CT), green is diesel (DS), blue is hydroelectric (HD), cyan is nuclear (NU), magenta is steam turbine (ST).

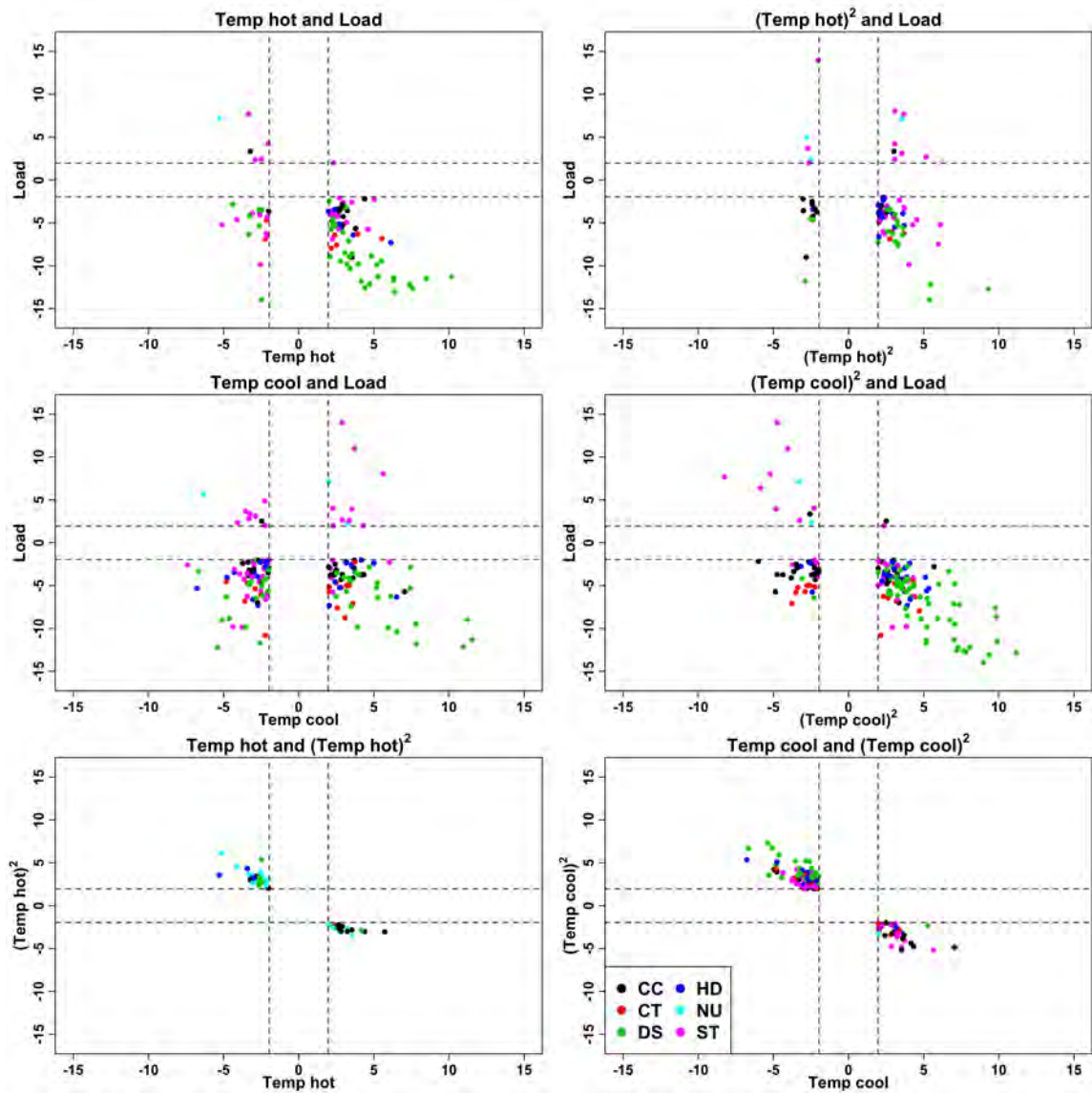


Figure B.10: Summarizing t -value relationships for non-orthogonal covariate pairs for the derated model (2004-2018 model fits). Thresholds for significance at 0.05 level (± 1.96) indicated by dashed lines. To be included in a plot in this figure, both relevant covariates must be present in the final derated model. Black is combined cycle gas (CC), red is simple cycle gas (CT), green is diesel (DS), blue is hydroelectric (HD), cyan is nuclear (NU), magenta is steam turbine (ST).

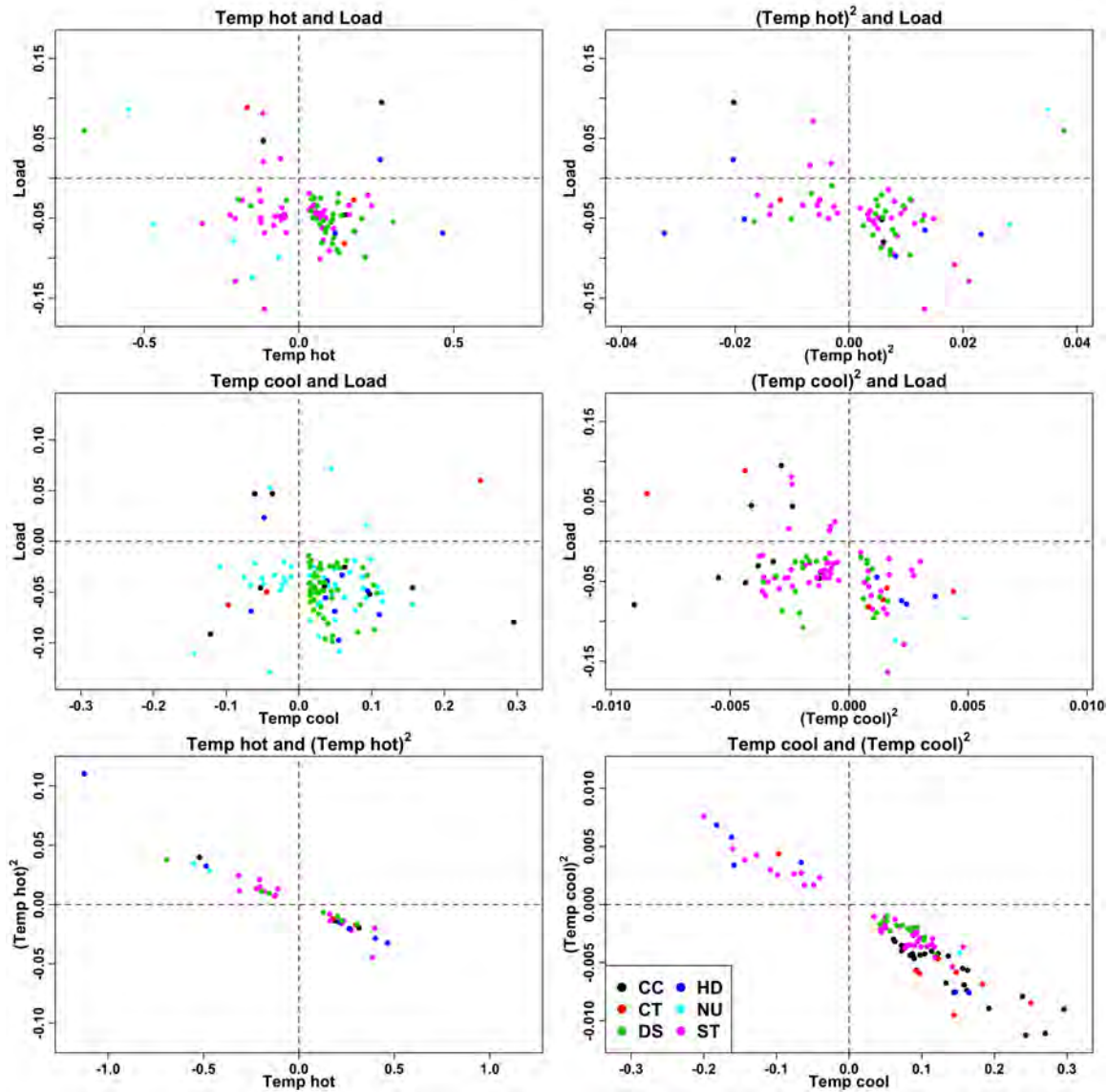


Figure B.11: Summarizing coefficient relationships for non-orthogonal covariate pairs for the available model (2004-2018 model fits). To be included in a plot in this figure, both relevant covariates must be present in the final available model. Black is combined cycle gas (CC), red is simple cycle gas (CT), green is diesel (DS), blue is hydroelectric (HD), cyan is nuclear (NU), magenta is steam turbine (ST). Dashed lines indicate 0. Temperature units are degrees C. Load units are GW. Axis scales set independently in each plot.

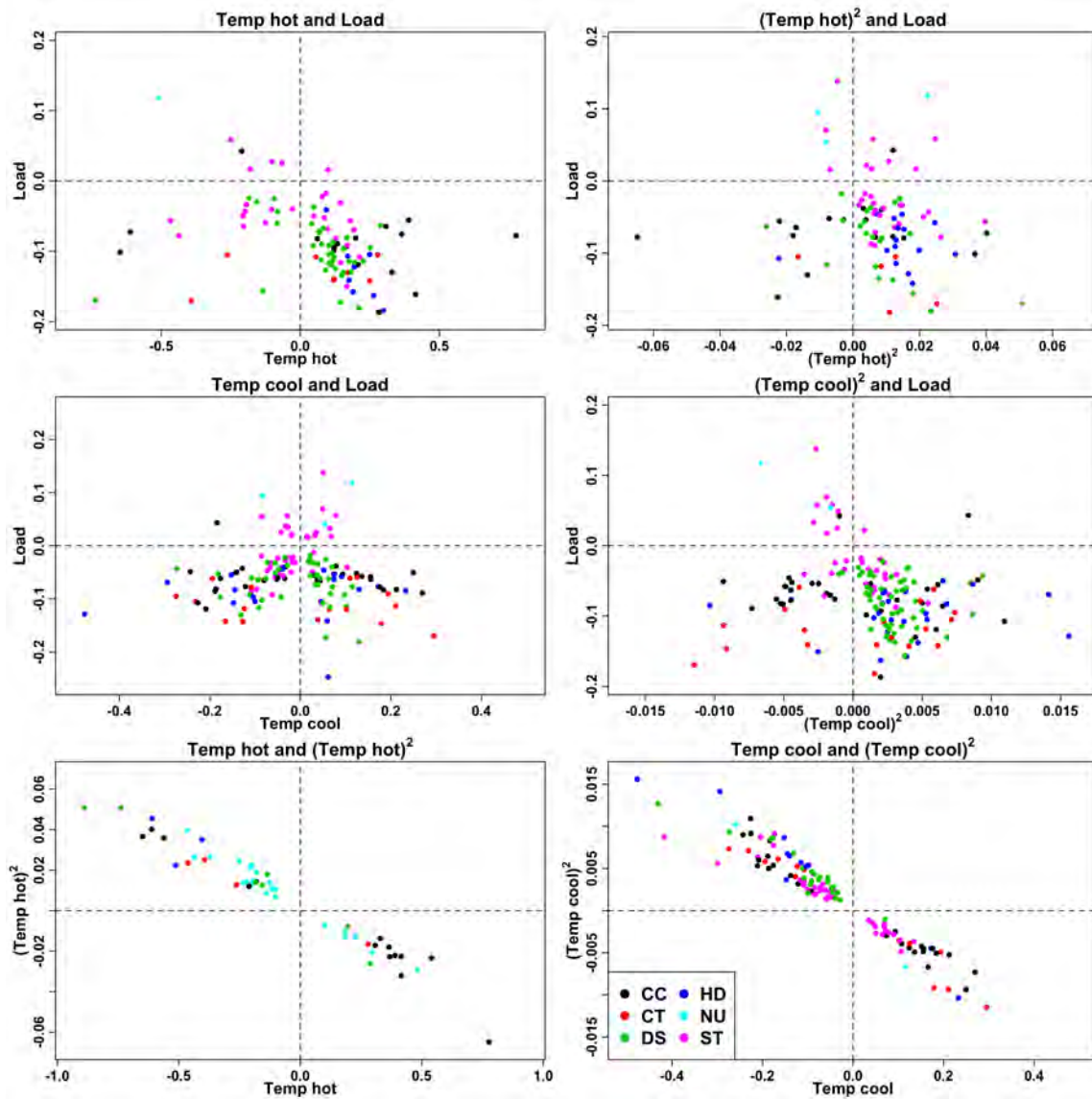


Figure B.12: Summarizing coefficient relationships for non-orthogonal covariate pairs for the derated model (2004-2018 model fits). To be included in a plot in this figure, both relevant covariates must be present in the final derated model. Black is combined cycle gas (CC), red is simple cycle gas (CT), green is diesel (DS), blue is hydroelectric (HD), cyan is nuclear (NU), magenta is steam turbine (ST). Dashed lines indicate 0. Temperature units are degrees C. Load units are GW. Axis scales set independently in each plot.

Model	0	1	2	3	4	5	6	7
Available	0	0	141	282	184	110	28	3
Derated	0	0	150	237	169	145	42	5

Table B.5: Number of statistically significant parameters (including constants) for the 748 generators with at least 10 instances of the less-common transition per parameter in both available and derated models (2004-2018 model fits).

Model	0	1	2	3	4
Available	287	247	166	41	7
Derated	263	233	187	57	8

Table B.6: Number of statistically significant temperature parameters (excluding constants) for the 748 generators with at least 10 instances of the less-common transition per parameter in both available and derated models (2004-2018 model fits).

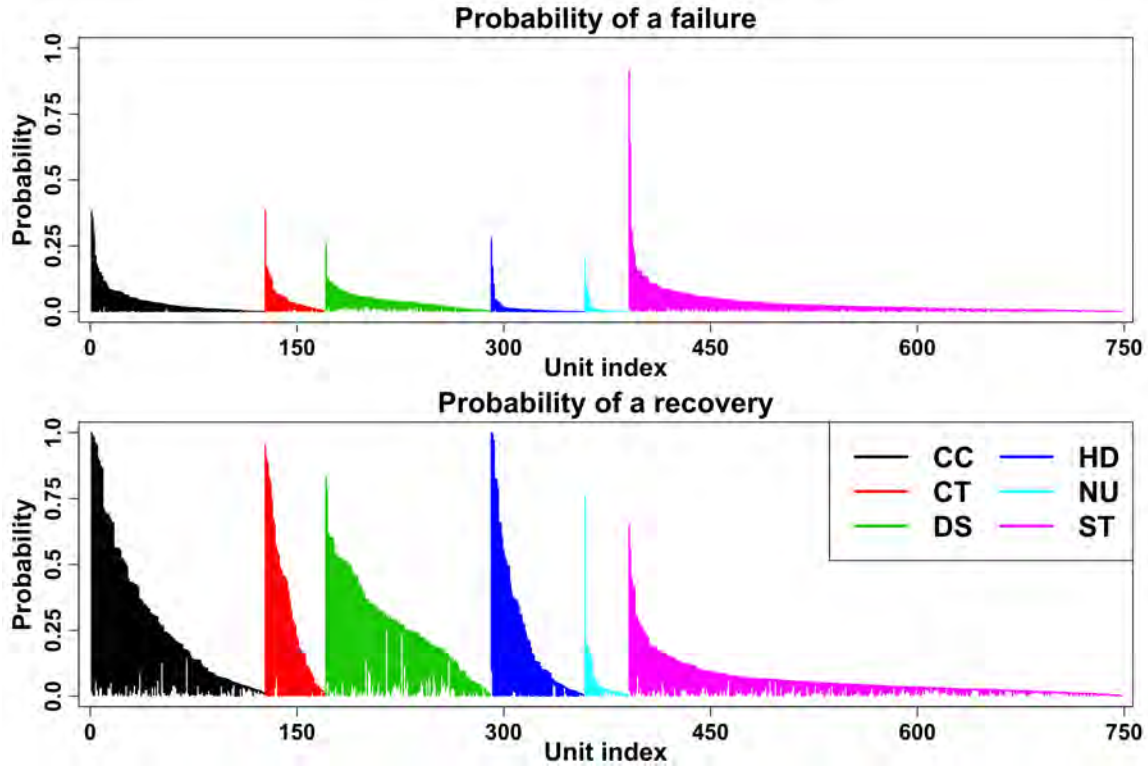


Figure B.13: Summarizing the empirical range of hourly transition probabilities (2004-2018 model fits). Plots include 748 generators with at least 10 failure and recovery events per statistically significant model parameter. Each generator is represented as a vertical line at an integer index (1 to 748). In each plot, generators are sorted by generator type and maximum experienced transition probability. Black is combined cycle gas (CC), red is simple cycle gas (CT), green is diesel (DS), blue is hydroelectric (HD), cyan is nuclear (NU), magenta is steam turbine (ST).

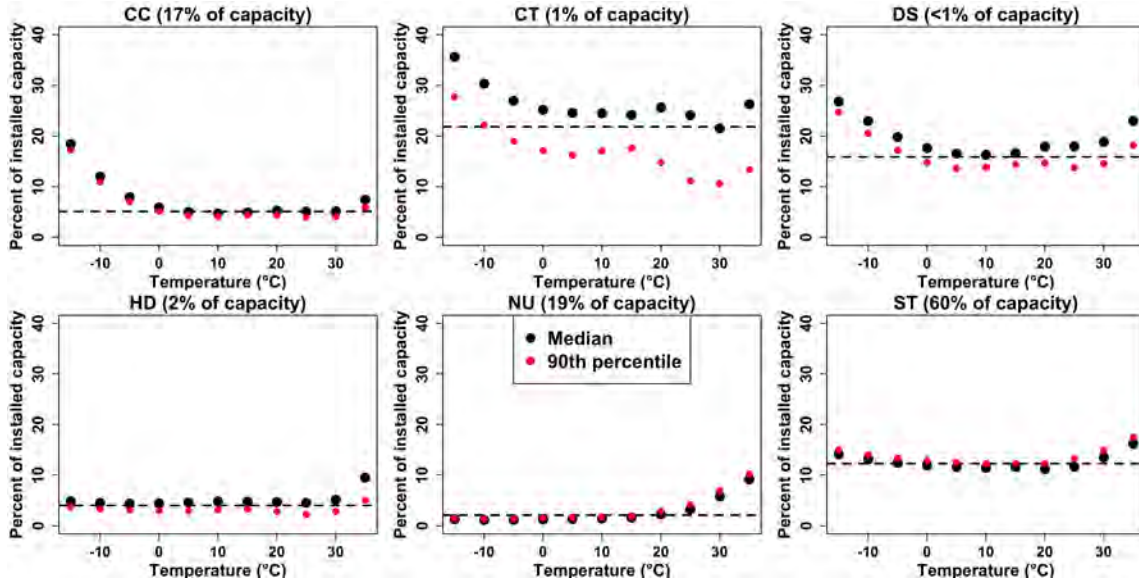


Figure B.14: Expected levels of unavailable capacity under logistic regression (dots) and current practice (dashed horizontal line), as a function of temperature (2004-2018 model fits). Black dots calculated using median load from temperature neighborhood, red dots calculated using 90th percentile load from temperature neighborhood. Temperature neighborhood is defined as ± 10 degrees. Not all generators experience full temperature range; see Figure B.15 for prevalence of temperatures. CC is combined cycle, CT is simple cycle, DS is diesel, HD is hydroelectric and pumped storage, NU is nuclear, ST is steam turbine.

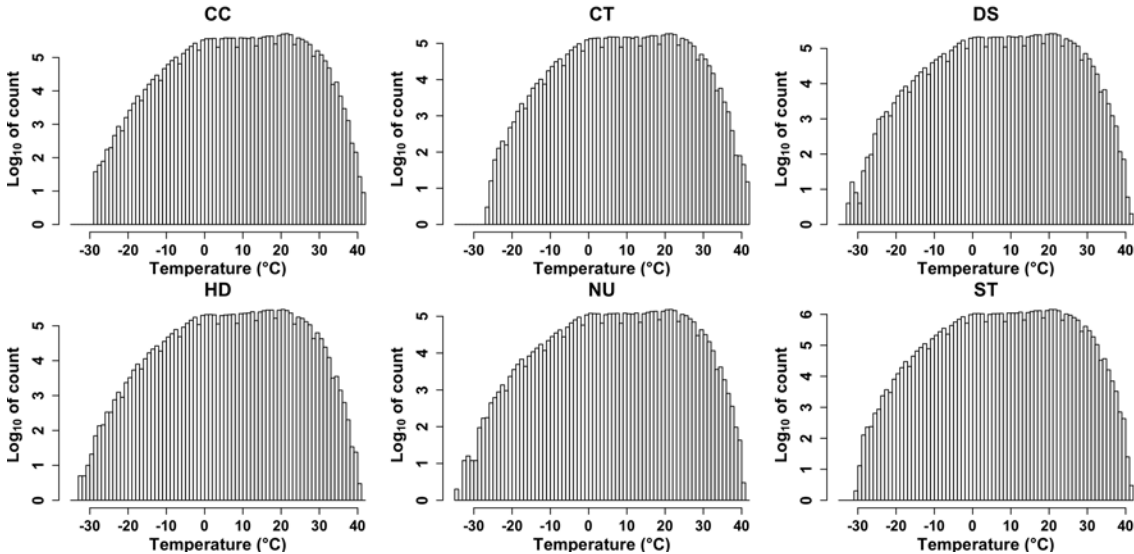


Figure B.15: Prevalence of temperatures experienced by 748 modeled generators by generator type (2004-2018 model fits). For use in conjunction with Figure B.14. Note the log scale on the ordinate. CC is combined cycle, CT is simple cycle, DS is diesel, HD is hydroelectric and pumped storage, NU is nuclear, ST is steam turbine.

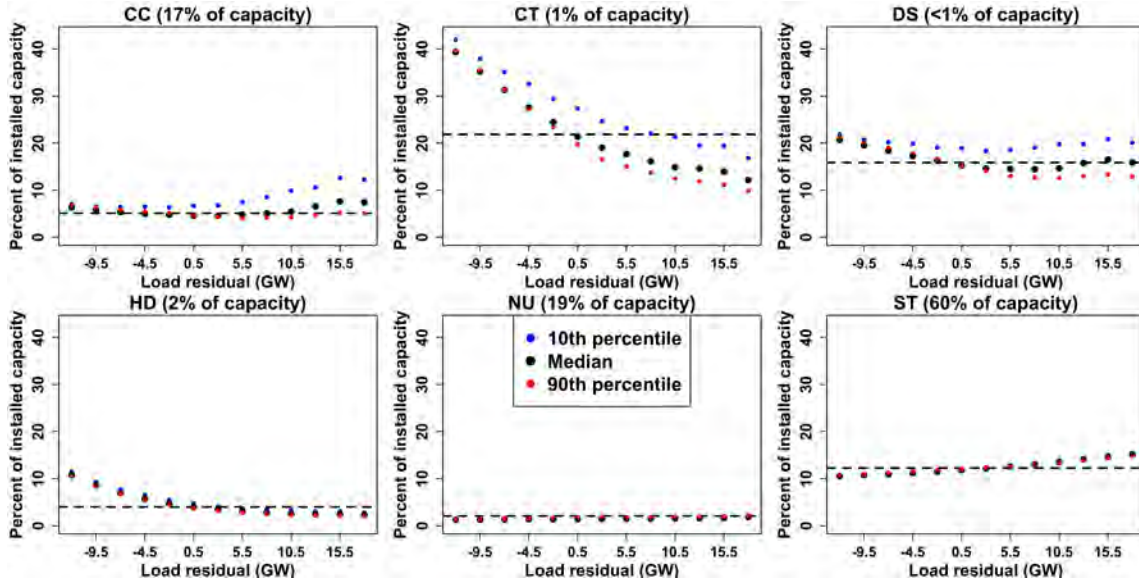


Figure B.16: Expected levels of unavailable capacity as a function of load under logistic regression (dots) and current practice (dashed horizontal line) when restricting to temperatures below 18.3 degrees Celsius (2004-2018 model fits). Black dots computed at median temperature from load neighborhood; blue and red dots correspond to 10th and 90th percentile temperatures from load neighborhood, respectively. Load neighborhood defined analogously to temperature neighborhood of Figure B.14. Current practice dashed line matches that of Figure B.14. Plot domain defined using only observations below 18.3 degrees. Abscissa spans different values than Figure A.14 because load stationarizing procedure computed independently for 2004-2018 model fit. CC is combined cycle, CT is simple cycle, DS is diesel, HD is hydroelectric and pumped storage, NU is nuclear, ST is steam turbine.

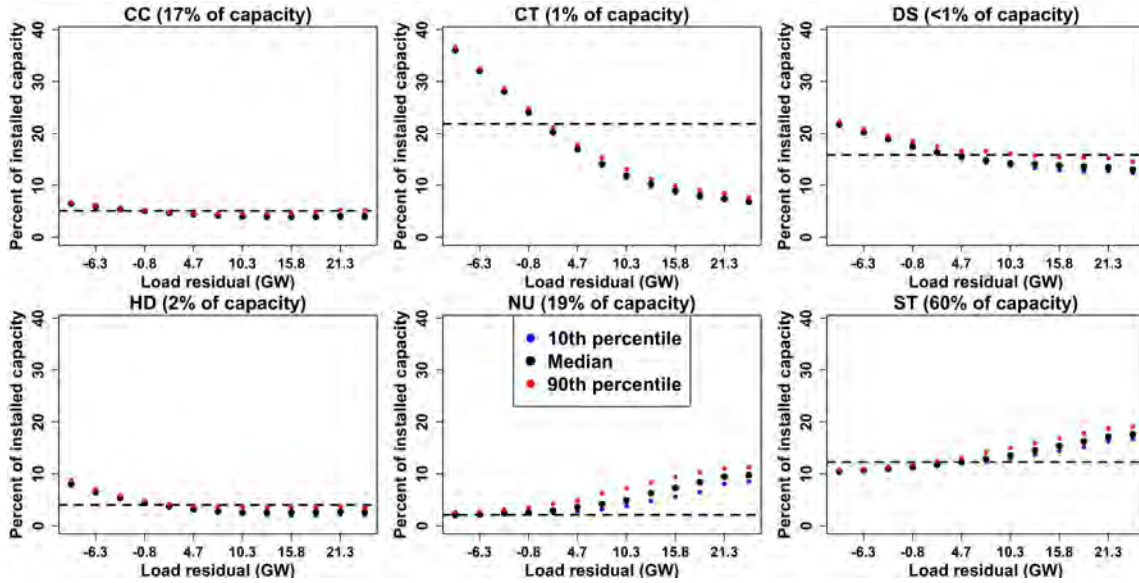


Figure B.17: Expected levels of unavailable capacity as a function of load under logistic regression (dots) and current practice (dashed horizontal line) when restricting to temperatures above 18.3 degrees Celsius (2004-2018 model fits). Black dots computed at median temperature from load neighborhood; blue and red dots correspond to 10th and 90th percentile temperatures from load neighborhood, respectively. Load neighborhood defined analogously to temperature neighborhood of Figure B.14. Current practice dashed line matches that of Figure B.14. Plot domain defined using only observations above 18.3 degrees. Abscissa spans different values than Figure A.15 because load stationarizing procedure computed independently for 2004-2018 model fit. CC is combined cycle, CT is simple cycle, DS is diesel, HD is hydroelectric and pumped storage, NU is nuclear, ST is steam turbine.